The Design and Optimization of a Lithium-ion Battery Direct Recycling Process

Panni Zheng

Thesis submitted to the Faculty of the Virginia Polytechnic Institute and State University in partial fulfillment of the requirements for the degree of

Master of Science

In

Mechanical Engineering

Zheng Li

Rui Qiao

Michael W Ellis

June 17th 2019

Blacksburg, VA

Keywords: Battery recycling, Lithium Cobalt Oxide, Lithiation

The Design and Optimization of a Lithium-ion Battery Direct Recycling Process

Panni Zheng

Abstract

Nowadays, Lithium-ion batteries (LIBs) have dominated the power source market in a variety of applications. Lithium cobalt oxide ($LiCoO_2$) is one of the most common cathode materials for LIBs in consumer electronics. The recycling of LIBs is important because cobalt is an expensive element that is dependent on foreign sources for production. Lithium-ion batteries need to be recycled and disposed properly when they reach end of life (EOL) to avoid negative environmental impact. This project focuses on recycling cathode material ($LiCoO_2$) by direct method. Two automation stages, tape peeling stage and unrolling stage, are designed for disassembling prismatic winding cores. Different sintering conditions (e.g., temperature, sintering atmosphere, the amount of lithium addition) are investigated to recycle EOL cathode materials. The results show that the capacity of the recycled cathode materials increases with increasing temperature. The extra Li addition lead to worse cycling performance. In addition, sintering atmosphere has little influence on small- scale sintering. Also, most of directly recycled cathode materials have better electrochemical (EC) performance than commercial $LiCoO_2$ (LCO) from Sigma, especially when cycling with 4.45V cutoff voltage.

The Design and Optimization of a Lithium-ion Battery Direct Recycling Process

Panni Zheng

General Audience Abstract

Nowadays, Lithium-ion batteries (LIBs) have dominated the power source market in a variety of applications. A LIB contains an anode, a cathode and electrolyte. The cathode material is the most valuable component in the LIB. Lithium cobalt oxide ($LiCoO_2$) is one of the most common cathode materials for LIBs in consumer electronics. The recycling of LIBs is important because cobalt is an expensive element that is dependent on foreign sources for production. Lithium-ion batteries need to be recycled and disposed properly when they reach end of life (EOL) to avoid negative environmental impact. The direct recycling is a cost effective and energy conservative method which can be divided into two steps: retrieving the cathode materials from EOL LIBs and regenerating the cathode materials. This project focuses on recycling $LiCoO_2$ by direct method. Two automation modules, tape peeling stage and unrolling stage, are designed for a disassembling line which is the automation line to collect the cathodes materials. The EOL cathode materials is lithium deficient ($Li_{1-x}CoO_2$). To regenerate the EOL cathode materials, lithium is added into structure of cathode materials which is called the re-lithiation process. The different sintering conditions (e.g., temperature, sintering atmosphere, the amount of lithium addition) are investigated for the re-lithiation process. The results show that the capacity of the recycled cathode materials increases with increasing temperature. The extra Li addition in

$Li_{1-x}CoO_2$ leads to worse cycling performance. In addition, sintering atmosphere has little influence on small- scale sintering. Most of directly recycled cathode materials have better electrochemical (EC) performance than commercial $LiCoO_2$, especially when cycling with 4.45V cutoff voltage.

Acknowledgements

I would like to appreciate my academic advisor, Dr. Zheng Li for providing experimental resources, academic guidance and continuous supports in my Master's career. I would also like to thank Dr. Rui Qiao and Dr. Michael Ellis for their support, comments and willingness to be my committee members.

I would like to acknowledge all my labmates, Dr.Sanpei Zhang, Dr.Heng Yang, Liurui Li, Tairan Yang, Dayang Ge, Qiaoyi Zheng, Yingqi Lu for providing necessary help on my experiments.

Finally, I would like to thank my family and all my friends for their encouragement and supporting.

Table of Contents

List of Figures

Chapter 1: Introduction and Background

1.1 Motivation

In recent years, LIBs required by the portable electronic devices and electric vehicles increase dramatically. The rapid growth of LIBs requires a significant amount of metal resources, especially lithium (Li) and cobalt (Co). Figure 1 shows demand for electric vehicle batteries from 2008 to 2020. The green line that represents the lithium demand from vehicle indicates that the demand of lithium would grow faster in the future. However, worldwide cobalt and lithium production have only increased slightly in recent years. Comparing current growth rates of demand and production, it is rational to predict that Co and Li would face a serious shortage in the future. Thus, the recycling can reduce the shortage of resource.

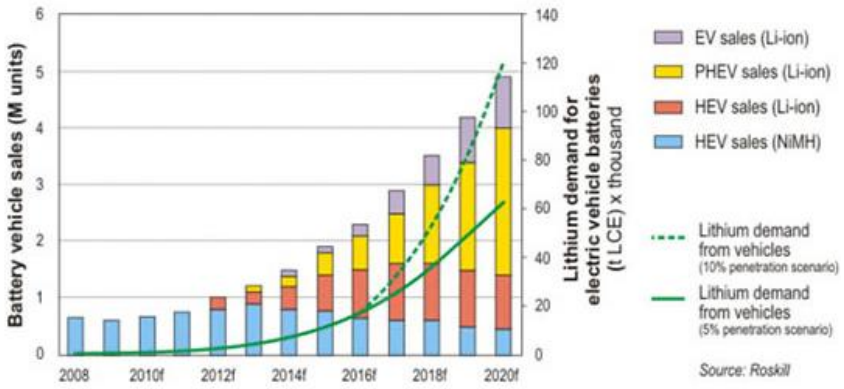

Figure 1. Lithium demand for electric vehicle batteries from 2008 to 2020[1]

Furthermore, the growing ubiquity of LIBs brings a rapid growth in end of life (EOL) battery that needs to be recycled. In the consumer electronics sector, there are over 1.2 billion shipments of smartphones globally since 2014 which implies 24,000 tons of lithium-ion battery cathode materials that need to be recycled in 2017 and roughly $1 billion in market size for the recycled materials. In the EV sector, approximately 2 million EV lithium-ion battery packs in the US and

China will reach their EOL by 2020 which translates to roughly 20,000 tons of EOL lithium-ion battery cathode materials and this recycling market growth will accelerate with the proliferation of EVs and the increasing use of lithium-ion batteries.

Figure 2. Spent LIB in Soil[2]

If spent LIBs disposed improperly, shown in Figure 2, the LIBs would have negative environmental impacts. The LIBs contain some metals like Co, Ni and Mn, which would contaminate soil and underground water. The electrolyte in LIB would easily react with water to release harmful gas such as hydrogen fluoride (HF). Additionally, during the cycle life period, Li tends to deposit on the anode due to overcharging or other improper usage. The deposited Li would react with water to release hydrogen gas (H_2) and produce lithium hydroxide (LiOH).[3] The Equation below displays chemical reaction of Li and water.

$$2Li + 2H_2O \rightarrow 2LiOH + H_2$$

Also, the residual electric power tends to cause explosions or fire accidents. Thus, developing the effective recycling of spent LIB can promote the sustainable development.

1.2 Construction of a pouch cell

There are a lot of manufactures producing the Li-ion batteries, and cylindrical, prismatic and so-called “polymer” are the most common types. For “polymer” Li-ion cell, originally, it has been defined that if the battery has a polymer or gel electrolyte. A Li-ion cell in a flexible aluminized polymer package is belong to “polymer” cell. Now, with the rapid growth of battery types, cells marketed today as “polymer” Li-ion cell are no more than a regular Li-ion cell in a flexible aluminized polymer package, so the more accurate term is called “pouch” cell.[4] A pouch cell contains a core and a cover. The core contains positive and negative electrodes, positive and negative tabs, separators and films (Figure 3). The positive tab is made of Al while the negative tab is made of Ni. The positive and negative tabs are attached to positive and negative electrode respectively and protrude from package cover. The cover is made of aluminum laminated film that is heat-sealable. The cover usually consists of a tri-layer of polypropylene/Al foil/polypropylene that has been thermally laminated together. After putting core in the plastic case that has been pouched into a shape accommodated the size of core, two sides are heat-sealed and then electrolyte is added into the case. Finally, the top side is sealed under vacuum.

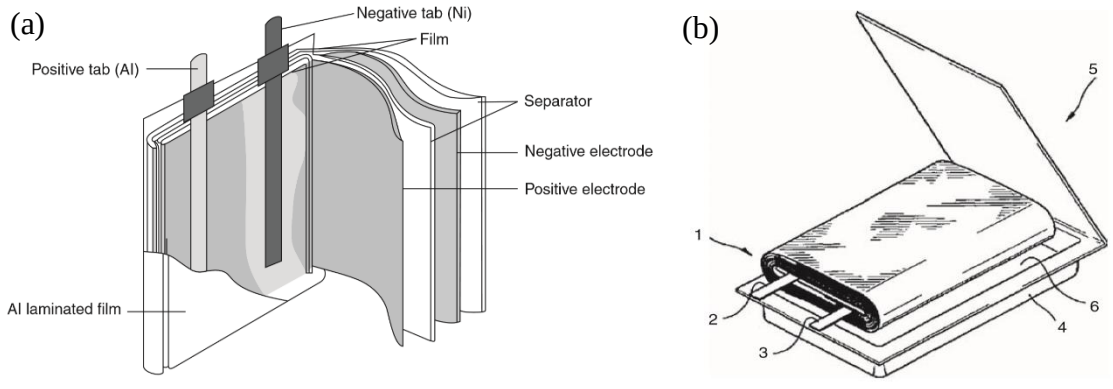

Figure 3.(a) Schematic diagram of a pouch Li-ion cell (b) The core (1) has protrude anode tabs (2) and cathode tabs (3). The aluminized film case (4) is pouched into the “pocket” shape to fit the core. The top cover (5) is heated sealed to the case (6)[4]

Figure 4 displays the fabrication process of Li-ion battery electrode. For positive electrodes, the slurry preparation process is mixing an active material, like $LiCoO_2$, a carbon-conductive additive, like acetylene black and a binder material, such as polyvinylidene difluoride (PVdF). The slurry is double coated on the current collector (Al foil). After drying the slurry, the electrodes are cut into predetermined length, pressed into predetermined thickness and calendared into predetermined width. Finally welding the tab on the current collector. Same process is applied for negative electrodes, but with different active material and different current collector (Cu foil).

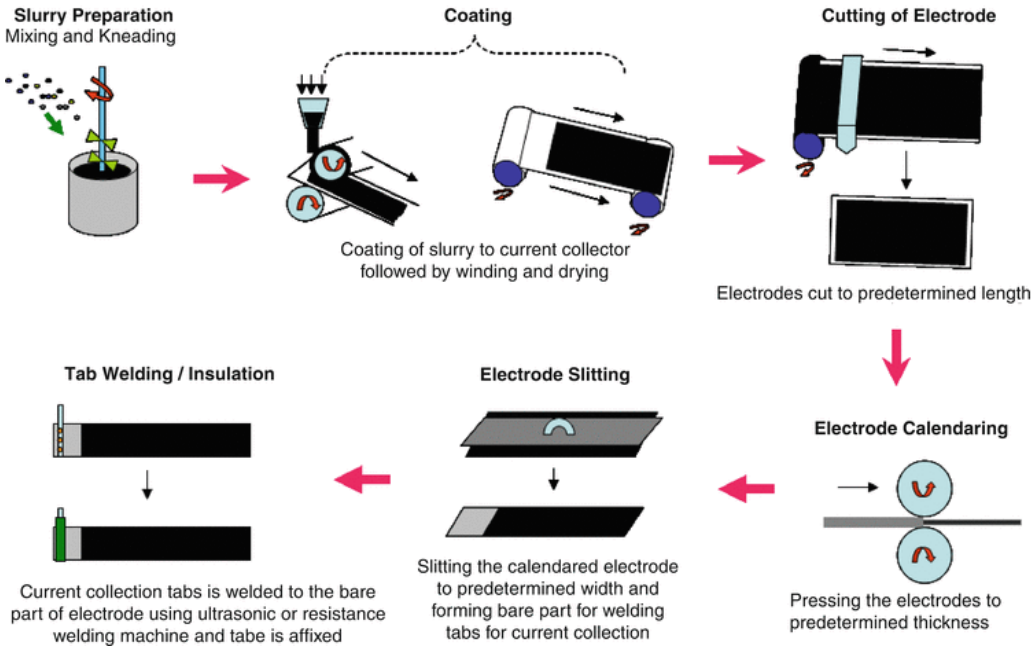

Figure 4. Schematic of Li-ion battery electrode fabrication process[5]

The prepared positive and negative electrodes and separators are used to make core. In the market, there are different types of cores depending on the different process methods, like z-folding, prismatic winding and single sheet stacking (Figure 5). In prismatic winding, four layers, a separator, a cathode, another separator and an anode are stacked together in sequence

and wound around flat mandrel. After winding mandrel is extracted, the core is compressed into prismatic shape. In the single stacking method, the electrodes and separator are cut into single sheets and stacked together alternatively. In Z-fold method, the electrodes are cut into single sheets, but separator is continuous. The single electrode sheets are folded into continuous separator. Tapes usually would be used to seal the end of core.

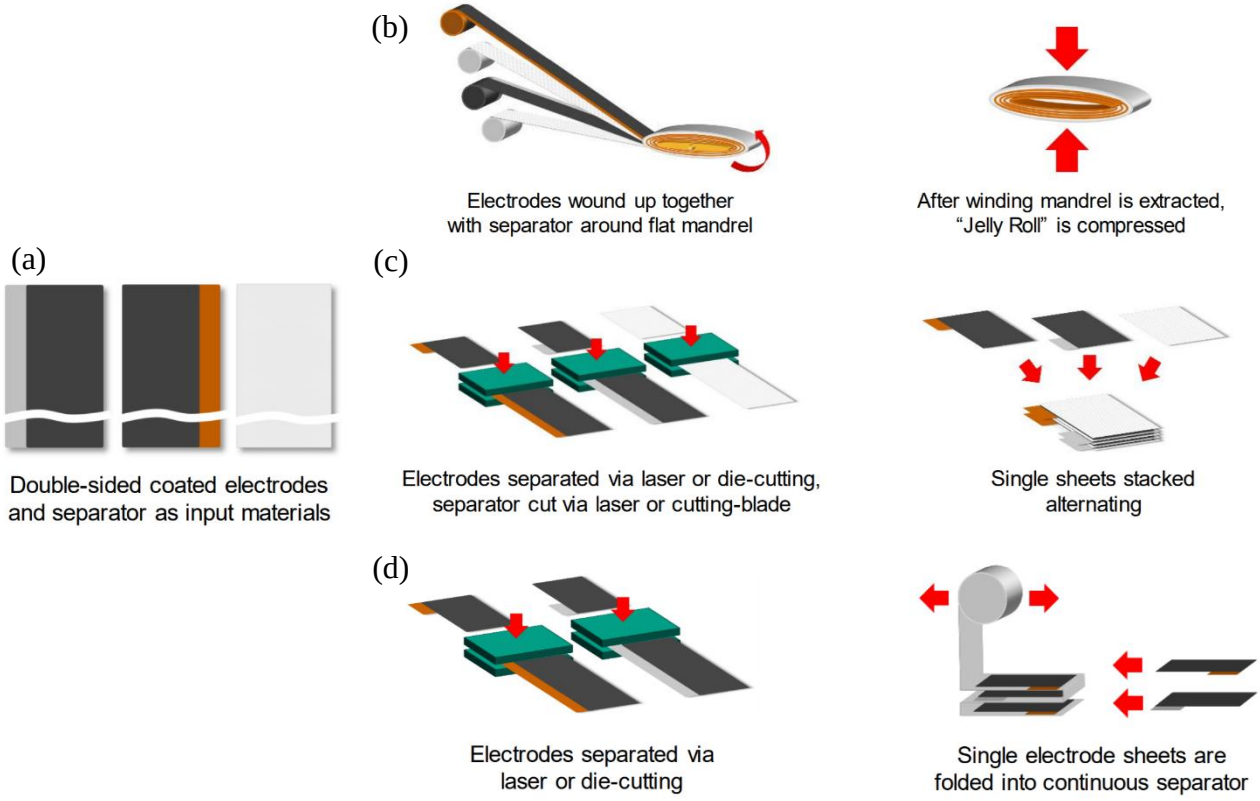

Figure 5. Schematic of (a)Prepared double coated electrodes and separators. (b)prismatic wending (c)single stacking and (d)z-folding process[6]

1.3 Principle of Li-ion Batteries (LIBs)

Lithium is an ideal material to make battery because of low density, relatively high reduction potential and kind of large energy density for weight. Li-based cells are most compact ways of

storing electrical energy. The energy density of LIBs is twice that of standard nickel-cadmium batteries.

A Li-ion battery is an energy conversion device that transfers the chemical energy to the electrical energy and vice versa by electrochemical oxidation-reduction (redox) reaction. Components in the battery include an anode, a cathode, an electrolyte and a separator. The anode works as source of lithium ions while the cathode is the sink of lithium ions. The electrolyte, which is the ionic conductor, provides the medium for the transfer of charge between the anode and the cathode. The separator, porous material that allows flowing of lithium ions, physically separates the anode and cathode to prevent an electrical short. The difference between chemical potential of li-ion in the anode and the cathode determines the cell's theoretical voltage and can be calculated by equation of Gibbs free energy:

$$\Delta G = -nFE$$

Where ΔG is Gibbs free energy; F is Faraday constant (9.649×10^4 C/mol); E is standard potential and n is the number of electrons transferred in reaction (n=1 for Li).

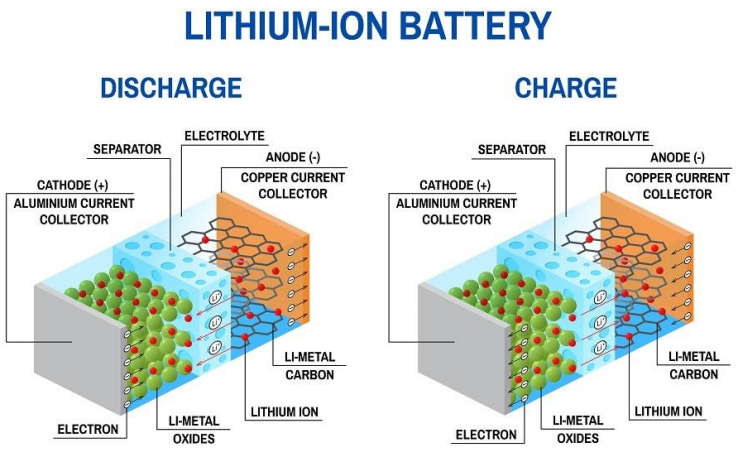

Figure 6. Lithium-ion battery's components and working principal[7]

Figure 6 displays all the components and how li-ions move during charging and discharging process. During discharging, the anode is reducing electrode that gives up electrons to external circuit and the cathode is oxidizing agent that accepts electrons from the external circuit. The graphite is the most common anode material for LIBs and the cathode material can be lithiated metal oxide or lithiated metal phosphate. The reaction on discharge can be written as follows:

Anode (Negative, oxidized, loss electrons): $Li_yC \rightarrow C + yLi^+ + ye^-$

Cathode (Positive reduced, gain electrons): $Li_{1-x}MO_2 + xLi^+ + xe^- \rightarrow LiMO_2$

Conversely, in charging process, the anode is oxidizing agent and the cathode is reducing agent.

Anode (Negative, reduced, gain electrons): $C + yLi^+ + ye^- \rightarrow Li_yC$

Cathode (Positive, oxidized, loss electrons): $LiMO_2 \rightarrow Li_{1-x}MO_2 + xLi^+ + xe^-$

In summary, during the discharging process (decreasing voltage), the li-ions are extracted from graphite (anode) and inserted into metal oxide (cathode). Conversely, during the charging process (increasing voltage), the li-ions are extracted from metal oxide (cathode) and inserted into graphite (anode). In other word, with respect to the cathode, delithiation (removing of lithium) leads to the cell voltage increase while lithiation (inserting of lithium) causes the cell voltage decrease.

During the discharging and charging processes, the graphite and metal oxide work as the host. The li-ions are removed from one side and inserted into another side, reversibly, without structure change to host. This progress called intercalation process. The graphite has layered structure that allow the intercalation process. Thus, the positive materials should also have the structure that allow the intercalation process. In the LIBs, a lot of different positive materials

have been developed. The positive materials can be divided into three structure types: an ordered rock salt structure, a spinel-type structure and an olivine-type structure, [4] (Figure 7).

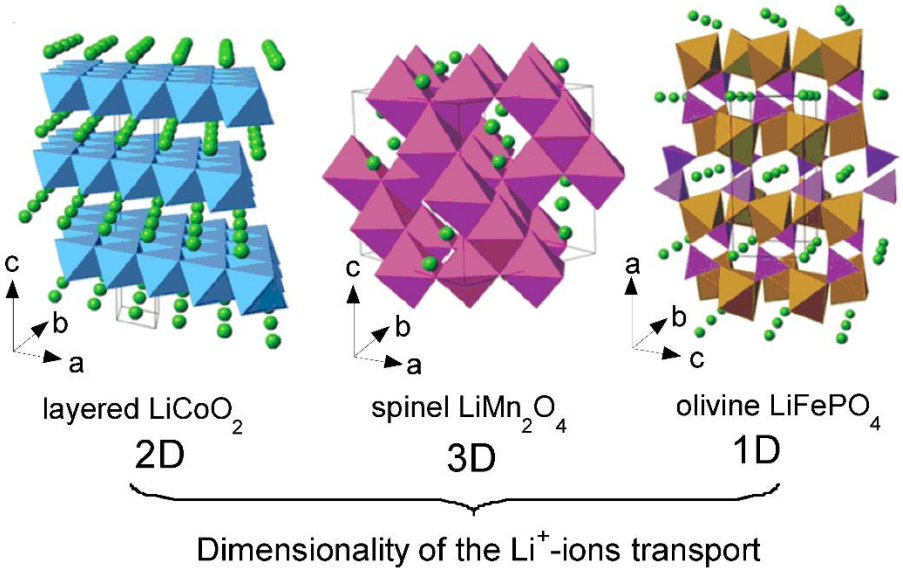

Figure 7. Three different crystal structures of lithium-insertion compounds[8]

My project is focusing on the LCO which has the layered 2D crystal structure.

1.4 Background and Basic Knowledge of LCO

Goodenough and Mizushima developed LCO and claimed that LCO was a feasible cathode material in 1980. They recognized that LCO had a layered structure and the lithium could be removed electrochemically.[9] SONY made the first marketed Li-ion batteries by combining the LCO cathode with a carbon anode in 1991.

1.4.1 Characteristics and X-ray powder diffraction (XRD)

Li_xCoO_2, when x equal 1, $LiCoO_2$ has the α-$NaFeO_2$ structure with the oxygens in a cubic closed-packed arrangement.[10] It has a 2D crystal structure which is showed in Figure 8. After

lithium is fully removed, the oxygen layer in this structure rearranges to be the hexagonal closed packing in CoO_2.

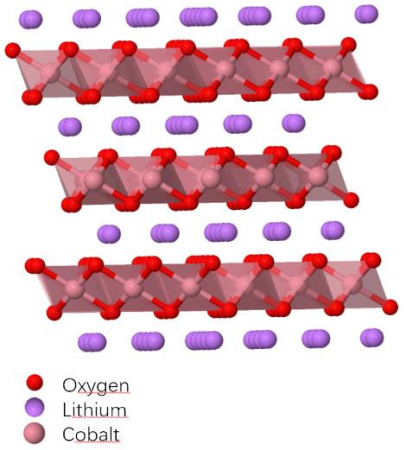

Figure 8. Layered crystal structure of LiCoO2

The XRD is a test to detect the crystal structure of materials. The XRD card of $LiCoO_2$ is 75-0532 XRD card. Figure 9 shows the XRD results from other groups with the standard card from ICDD data.

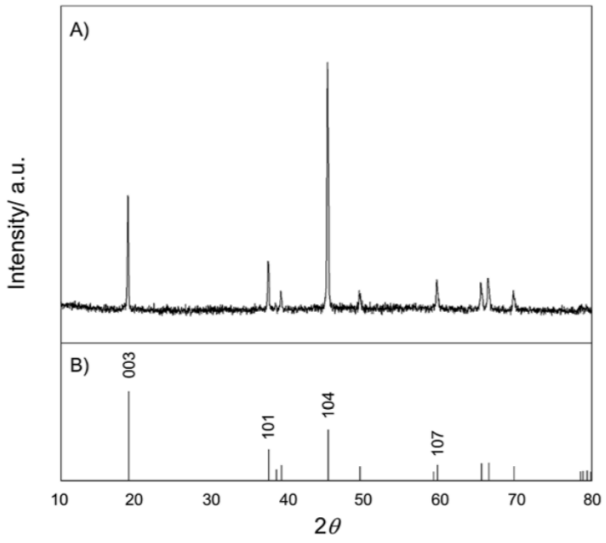

Figure 9. X-ray diffraction (XRD) profiles of (A) the as-obtained product and (B) ICDD data for LiCoO2 (PDF 75-0532)[11]

The peaks would change or shift when the structure changes. The XRD results in Figure 10 shows the 003 and 104 peak shifts with different voltages. When the voltage increases, the delithiation happens, and peaks shift to left and vice versa.

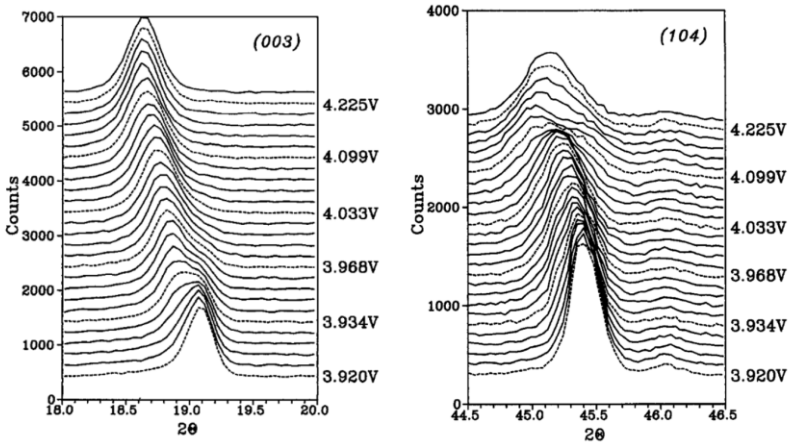

Figure 10. (003) and (104) peak shift verse voltage[12]

1.4.2 Physical Properties and Scanning Electron Microscope (SEM)

The materials' particle size and particle-size distribution, particle shape, particle specific surface area and tap density are important factors of LIBs' properties. The particle size controls the solid-state diffusion path length: the larger size, the longer path and take more time to delithiation from structure. The particle-size distribution determines the aspects of the rate capability and influence the properties of slurries. The interaction between materials and electrolyte would occur on the surface of particles. With larger specific surface area, the more interaction happens which influences the reactivity of charged materials with electrolyte at elevated temperature. Also, the tap density determines the ultimate density of electrode: the higher tap density, the larger ultimate density[4].

SEM can observe the properties of particles of materials. Figure 11 shows the SEM micrographs of LCO (produced by human Reshine New Material Co.). From images, the surface of LCO is

smooth. The mean particle size of $LiCoO_2$ (R757) is around 6.5 ~ 9.5 μm and around 9.0 ~14.0 μm for $LiCoO_2$ (R767). The specific surface area is 0.4 ~0.75 m^2/g for R757 and <0.45 for R767. The tap density of R757 is 2.1~2.9 g/mL and >2.5 g/ml for R767.[4]

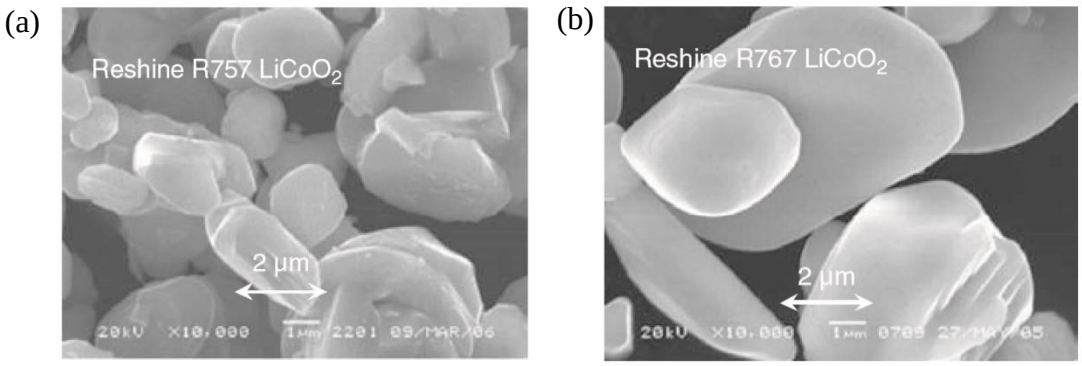

Figure 11. SEM images two different types of LiCoO2[4]

1.4.3 Electrochemical Properties

In the research process, the researchers usually assemble LCO with metallic lithium to test the properties of LCO. The charging and discharging process for a cell with LCO cathode can be expressed by following chemical reaction:

Discharging: $Li_{1-x}CoO_2 + xLi^+ + xe^- \rightarrow LiCoO_2$

$xLi^+ + xe^- \rightarrow Li$

Charging: $LiCoO_2 \rightarrow Li_{1-x}CoO_2 + xLi^+ + xe^-$

$Li \rightarrow xLi^+ + xe^-$

During lithiation (discharging) and delithiation (charging) processes, with different Li/Co value, the voltage also changes, displayed in Figure 12.

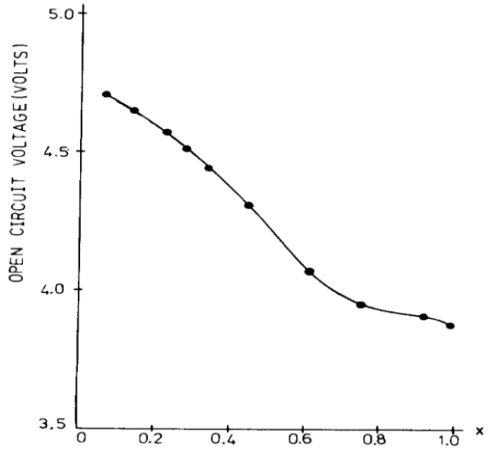

Figure 12. Open circuit voltage changes with different composition x for LixCoO2[9]

Figure 13 shows the discharging and charging profile of LCO. The charging and discharging curve have the plateau around 3.9V.

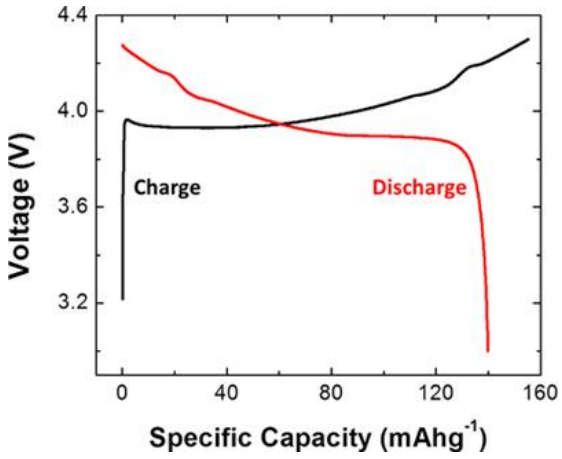

Figure 13. Charging and discharging profile of LCO

The theoretical capacity of $LiCoO_2$ is around 274mAh/g and can be calculated by the formula below:

$$Q_{\text{theoretical}} = \frac{nF}{M_w} = \frac{(1)(9.649 \times 10^4\ \text{C/mol})}{(97.87 g/mol)}\frac{1000}{3600} = 274\ mAh/g$$

Where n is number of ion transfer, F is Faraday constant and Mw is molecular weight. However, the practical specific capacity of $LiCoO_2$ is around 140 mAh/g. Figure 14 explains the reason: since $Co^{4+/3+}$ overlaps with O^{2-} oxidation potential, it will release oxygen when value of x is below 0.5 (when x=0.5, potential is around 4.2V). Although $LiCoO_2$ can deliver more capacity when charged to higher potential (higher than 4.2V), it would lead to bad cycle performance – capacity decay quickly.

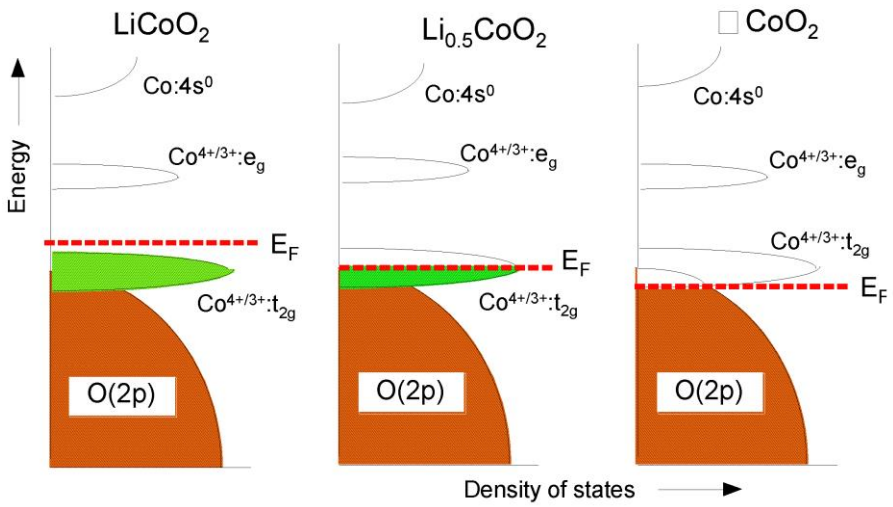

Figure 14. Qualitative energy diagrams of Li_xCoO_2 [13]

The real capacity of $LiCoO_2$ also depends on the charging and discharging rates which are governed by the C-rate. C-rate is defined as the charging/discharging current divided by the nominally rated battery capacity. For example, for 1C rate would deliver the battery's rated capacity in one hour; 2C rate means it would charge/discharge twice as fast (30min) and 1/2C rate means twice as slow (2 hours). The larger C-rate, the larger current and the shorter time it

takes to finish one cycle. With the larger C-rate, the real capacity would decrease as well. The higher C-rate requires faster electrons transfer, however the slow diffusion of Li-ion in electrode can't follow up, so the capacity decrease. Also, to keep equilibrium, the voltage is a compensated parameter. The voltage would decrease during the discharging process and increase during charging process. Figure 15 displays how current affects the capacity and voltage upon the discharge curve.

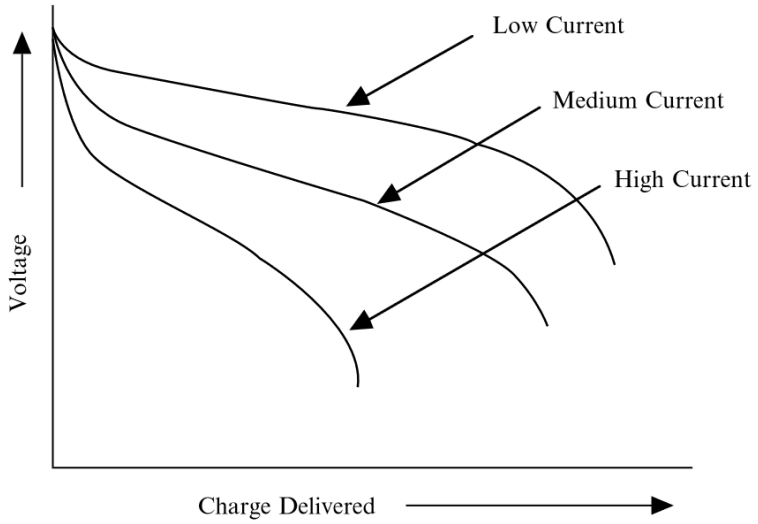

Figure 15. Effects of current density on the discharge curve[14]

1.4.4 Synthesis of LCO

For past several decades, a lot of synthesis methods of LiCoO2 have been developed. For example, the solid states synthesis which is high temperature treatment, and hydrothermal or solvothermal, microwave, intercalation, sol-gel, which are belong to the low temperature synthesis methods. With different synthesis methods, particle size, characterization, capacity, energy and EC performance are all different.

The solid-state synthesis is the oldest, the simplest and the most common method to prepare the solid material with mixed powdered reactants. $LiCoO_2$ was first discovered by John Bannister Goodenough's group and the synthesis method they used was solid state. They used the lithium carbonate (Li_2CO_3) and cobalt carbonate ($CoCO_3$) as original materials. The original materials were mixed together, and the mixture was pressed in to pellets. Then the pelletized mixture was heated under 900 ℃ for 20h in the air condition. Now, in general, researchers usually use the cobalt oxide or cobalt carbonate with lithium carbonate or lithium hydroxide (LiOH) and sintering in at 700℃ to 1000℃ in air. Normally, materials are made with a Li:Co stoichiometric ratio of 1:1 or with slight excess of lithium. The melt point is 723 ℃ for Li_2CO_3 and 462 ℃ for LiOH and 427 ℃ for $CoCO_3$.

1.5 Ageing mechanisms in LIBs

Although LIBs are widely used in our daily lives, one of the biggest problems of LIBs is that LIBs have lifespan and will reach the end of life. This section briefly introduces the reason for the ageing of LIBs. Ageing mechanisms occur at both anodes and cathodes, also at electrolyte and separators.

1.5.1 Ageing of Anodes

Anode ageing effects occur during the battery storage and using. Electrochemical properties are a good indicator of ageing in storage, like decay of capacity, rise of impedance, change of potential, state of charge and discharge. Ageing effects in the using include degradation, lithium metal plating, etc. The ageing effects may be caused by the changes of the electrode/electrolyte

interface and the electrolyte, the changes of active materials, and the change of the composite electrode (current collector, active material, binder, conductive additives, porosity, etc.)[15]

Figure 16 demonstrates the interface changes between anode electrode and electrolyte. The formation of SEI at the anode is accompanied by the gas releasing from electrolyte decomposition.[16] The formation of SEI is an irreversible reaction that consumes charge capacity. With the growth of SEI, the electrode impedance will increase. After SEI formation, anions, electrons and solvated cations, solvents and some impurities can still diffuse or migrate through SEI and the transport of solvated lithium cations and other components in the electrolyte can cause the dissolution and precipitation of SEI. In the later cycles, the lithium plating happens with subsequent corrosion. Consequently, the SEI penetrates into pores of electrode and into pores of separator, which cause a decrease of accessible active surface area of the electrode. [15]

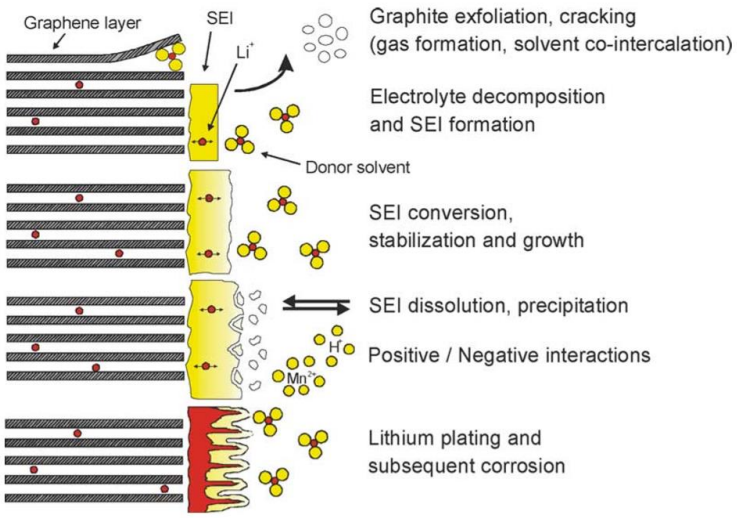

Figure 16. Changes of electrode/electrolyte interface[15]

For the active material in anode, during the inserting and removing of li-ions, the volume change is small, which has a little effect on reversibility. Also, the structure changes and redox reaction on the surface has minor effect. However, graphite exfoliation and graphite partials cracking due

to solvent co-intercalation, electrolyte reduction inside graphite, and/or gas evolution inside graphite will certainly lead to a rapid degradation of electrode.[15]

1.5.2 Ageing of Cathode

Similar to the ageing mechanisms of anode, the ageing mechanisms of cathode also influence the life span of cell. Figure 17 demonstrates basic ageing mechanisms that would happen on the cathode materials: ageing of active material, the degradation or changes of supply components of electrode, like corrosion of current collector, binder decomposition, oxidation of conducting agent, also corresponding oxidation of electrolyte components from formation of surface film and interaction between ageing products and negative electrode. The Figure 18 shows how those phenomena influence the performance of a cell.

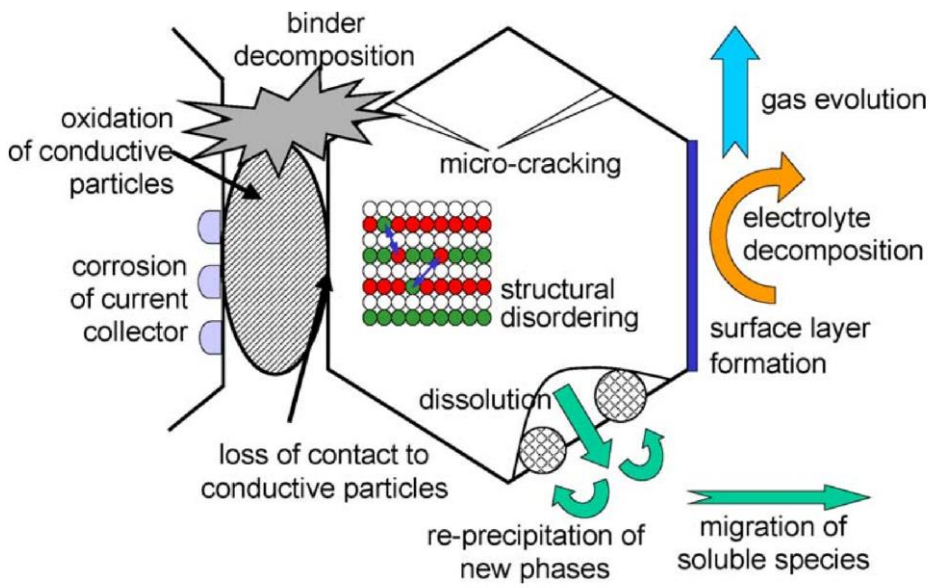

Figure 17. General ageing mechanism of cathode materials[15]

The decomposition of binder like polyvinylidene difluoride (PVdF), the oxidation of conductive agent like carbon, and the corrosion of current collector would cause the bad contact which results in the increasing of impendence. During charging and discharging process, li-ions

inserted in and extracted from the metal oxide repeatedly, which creates the mechanical stress and strain to the metal oxide, consequently causing the micro-cranking of the structure. Also, the phase transitions during the reaction would lead to the disorder of crystal lattice which increases the stress and strain in the structure. The cracking and disordering break the host structure, and the ability to contain li-ions reduce, which causes the capacity fading. Usually we represent EOL of lithium cobalt oxide as $Li_{1-x}CoO_2$ while x is missing lithium. With the continuous float charging, the free transition metal like free Co would be produced and be solved in electrolyte. The metal dissolution leads the decomposition of electrolyte and change the crystal structure. Also, the overcharging (x< 0.5 or voltage > 4.2V) would lead to the decomposition of electrolyte and active the O2p orbitals, releasing the gas.

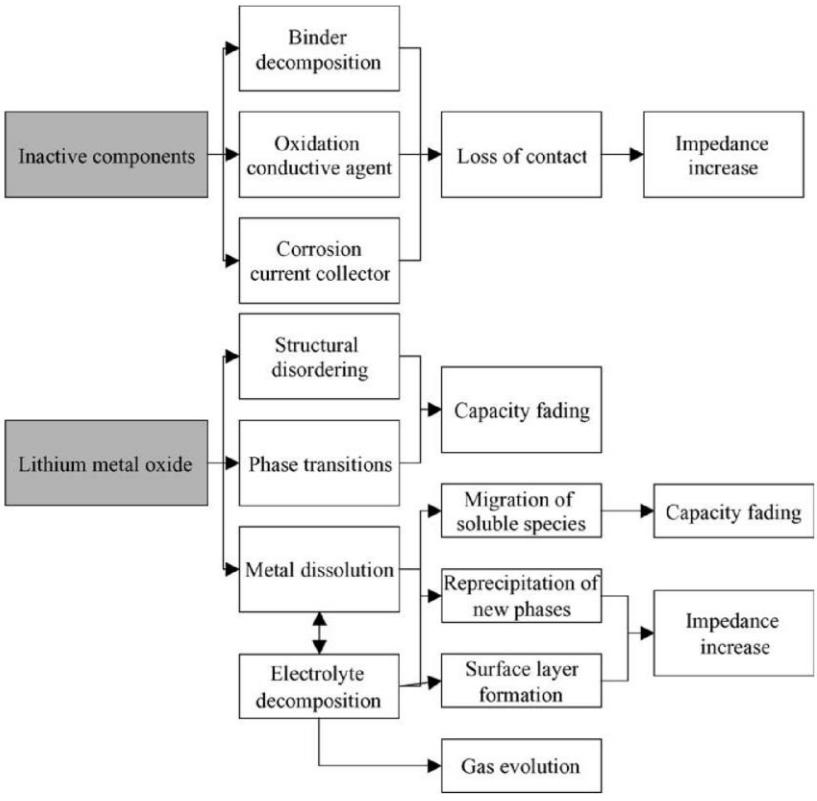

Figure 18. Origins and effects of various ageing mechanisms of Cathode material[15]

1.6 Direct and Indirect Recycling Method

For one LIB, the most valuable material of battery is cathode material. The most valuable component on LIB is cathode material, like $LiCoO_2$. Especially, Cobalt is an expensive element. Thus, recycling cathode material generates most value.

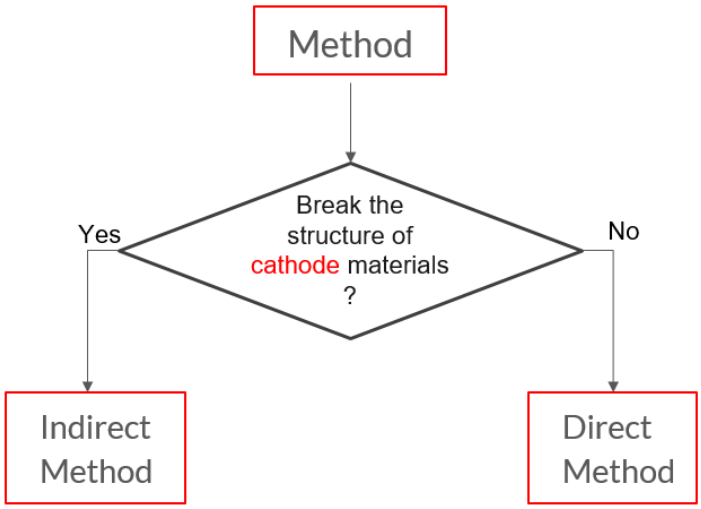

Figure 19.Difference between indirect and direct recycling method

Recycling method can be divided into two types, indirect and direct method, which can be define by checking if the structure of cathode material is breaking or not, as displayed in Figure 19. During recycling process, if cathode material is broken down to different elements, then the method is indirect method, otherwise it is direct method.

For indirect method, the final product is element constituents and for direct method, the final product is cathode material. Figure 20 shows the price of elemental constituents is around 19$/kg, but the cathode price is 40$/kg. The cathode material is much more expensive than elemental constituents, which means the structure of cathode materials is valuable. Thus, direct recycling methods are cost effective and energy conservative.

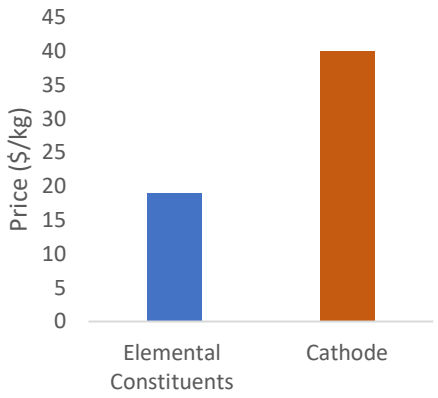

Figure 20. Elemental constituents vs. battery grade cathode materials of LCO

1.6.1 Indirect Method

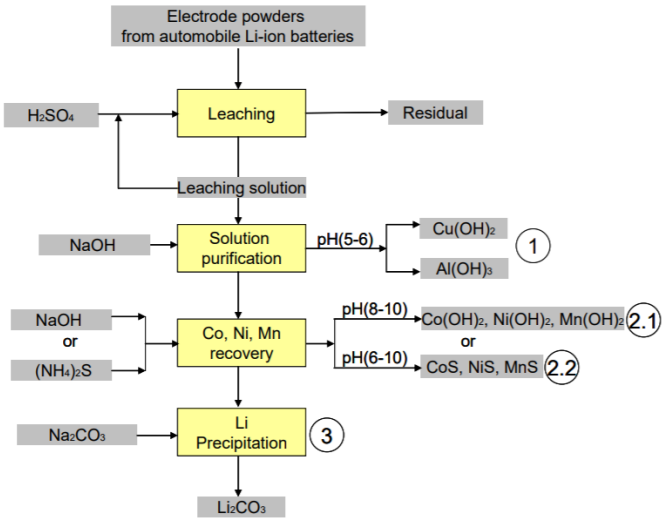

Figure 21. Diagram of hydrometallurgical recycling process[17]

The indirect method includes Pyrometallurgical and Hydrometallurgical method. The Figure 21 demonstrates a type of hydrometallurgical recycling process and steps include leaching, solution purification, Co, Ni, Mn recovery and then Li precipitation. The purpose of leaching process is that dissolving the valuable metals from raw material in leaching solution. In the solution purification step, copper and aluminum are removed first by hydroxide precipitation. The co-

precipitation and adsorption of Co/Ni in the precipitate is prevented as much as possible. With an appropriate temperature and reaction time, the equilibrium can be completely reached. The $Cu(OH)_2$ and $Al(OH)_3$ particles can grow and aggregate to the enough size. Subsequently, the solution can be filtered, and the residual is supplied to copper and aluminum production. At the moment, the Al and Cu are precipitated together, it will be tried to remove them from the solution separately in future.[17] By using the hydrometallurgical recycling method, the final lithium product is Li_2CO_3, which is the raw material used for $LiCoO_2$ synthesis. Further processes are needed to transfer Li_2CO_3 to $LiCoO_2$ by adding the $CoCO_3$.

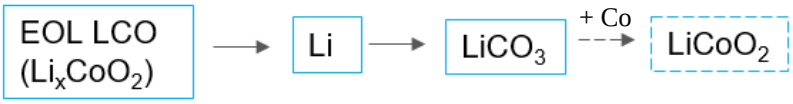

Figure 22. Processing path of lithium in hydrometallurgical recycling process

Figure 22 displays how lithium elements become different products in the recycling process. During the progress, the Li_xCoO_2 first is decomposed to Li, which means the original structure of cathode material is destroyed. Therefore, this hydrometallurgical recycling process is the indirect method.

1.6.2 Direct Method

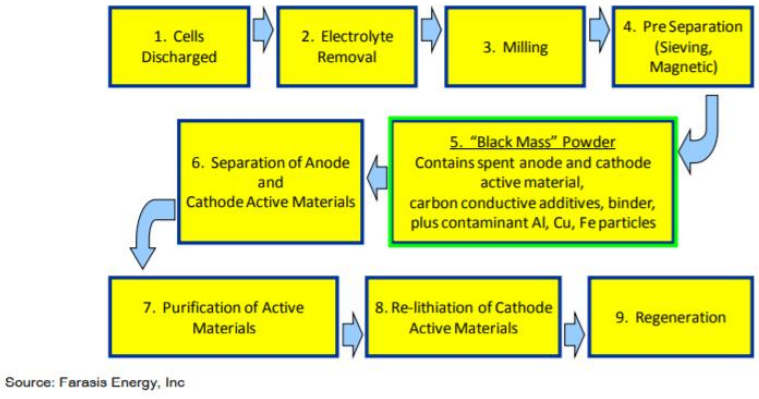

Figure 23. Direct recycling technology from farasis energy[18]

Figure 23 demonstrates a general flow chart for the direct recycling process by Farasis Energy. They first discharge a cell and remove electrolyte. Then entire cell is shredded by a milling machine and “black mass” powder is gained. The second step is separating active materials from “black mass” powder bases on the relative density difference between the anode material (graphite), and much denser transition metal oxide cathode materials. Finally, the active materials are purified and re-lithiated.

Figure 24. Processing Path of Lithium in direct recycling system

In the direct process, the final product is cathode material straightly: generates the $LiCoO_2$ directly from end of life LCO, as shown in Figure 24. Thus, the method is direct recycling method.

Nowadays, a lot of research are focus on the re-lithiation process. Farasis energy company mixes the lithium carbonate or lithium hydroxide with 0, 5, 15, and 25 present lithium added. The mixture is reacted in a high temperature furnace for an extended period. Figure 25 shows the capacity of recycled capacity, with 15% li addition, the capacity is around 140 mAh/g.

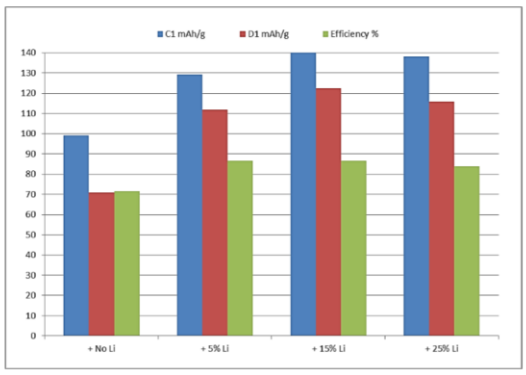

Figure 25. Optimization of Lithium Content in Recycled Cathode Materials from Farasis Energy[18]

Ultrasonic hydrothermal method is another re-lithiation process. In ultrasonic hydrothermal method, The EOL LCO are mixed with LiOH solution. The mixture is poured into the ultrasonic irradiation with stirring device. It was heated to 120 °C and ultrasonic generator power was set to 999 W (‘work 5 s–stop 2 s) and applied for 10h. Then the mixture is cool down to room temperature. The residue is washed several times with deionized water and dried at 80 °C until constant weight. Figure 26 displays the EC performance of recycled LCO with ultrasonic hydrothermal method. The capacity is around 132.6 mAh/g.

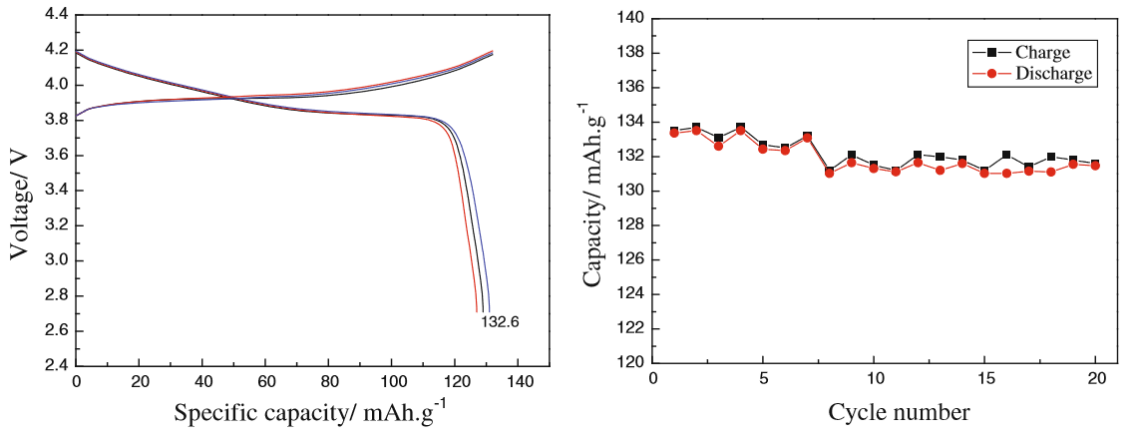

Figure 26. EC performance of recycled LCO with ultrasonic hydrothermal method[19]

1.7 Research Approach

My research is focusing on the recycling of EOL LCO pouch cell with prismatic winding core My research can be divided into two parts: designs of automation stages and recycling of cathode material (LCO). The method I choose is direct recycling by sintering the EOL LCO with LiOH. The objective is to study how the temperature, the atmosphere (Air and O_2) and impact of the amount of lithium addition influence the property of the LCO by compare the characterizing and EC performance. For the EC performance, I focus on testing the properties at high current (1C) with different cutoff voltages (3V~4.2V and 3V ~ 4.45V).

Chapter 2: Tape Peeling Stage and Unrolling Stage Design

In our lab, there is an automation battery disassembling line that has been designed for the pouch cells with z-folding cores (Figure 27). The system includes a pouch trimming module that cut the edge of a pouch cell, a pouch removal module that remove the cover and take out the core of the cell, the electrode sorting module that scrape the cathode and anode electrodes from separator and collected cathode and anode electrode separately. The pouch trimming, and pouch removal modules work for the pouch cells with different type of cores, but the electrode sorting module is not applicable for prismatic winding core. Thus, my project is designing several replaceable modules for disassembling prismatic winding core.

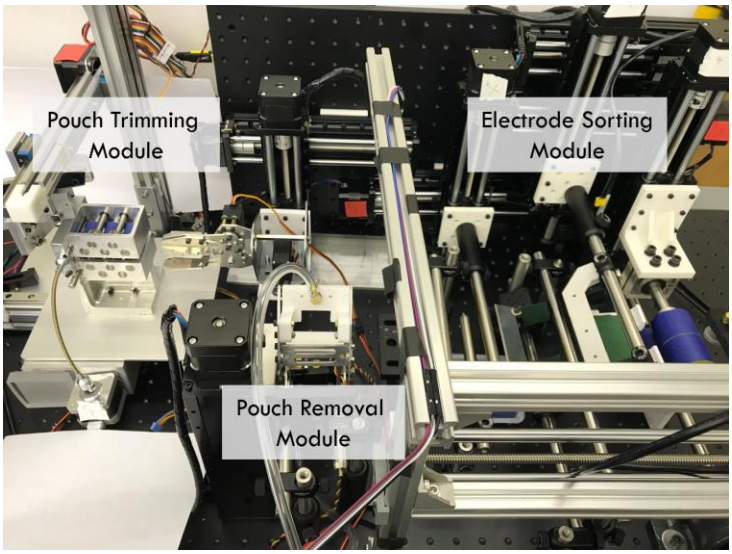

Figure 27. Existing automatic disassembling Line build for Z-folding core

The stages I designed are tape peeling and unrolling stage. The mechanical parts are purchased from the McMaster and Thorlab. The controller board include the Arduino Mega and SparkFun Stepoko which is Arduino compatible. The stages also include some 3D printer parts. Figure 28 displays the overview of 3D model of tape-peeling and unrolling stage.

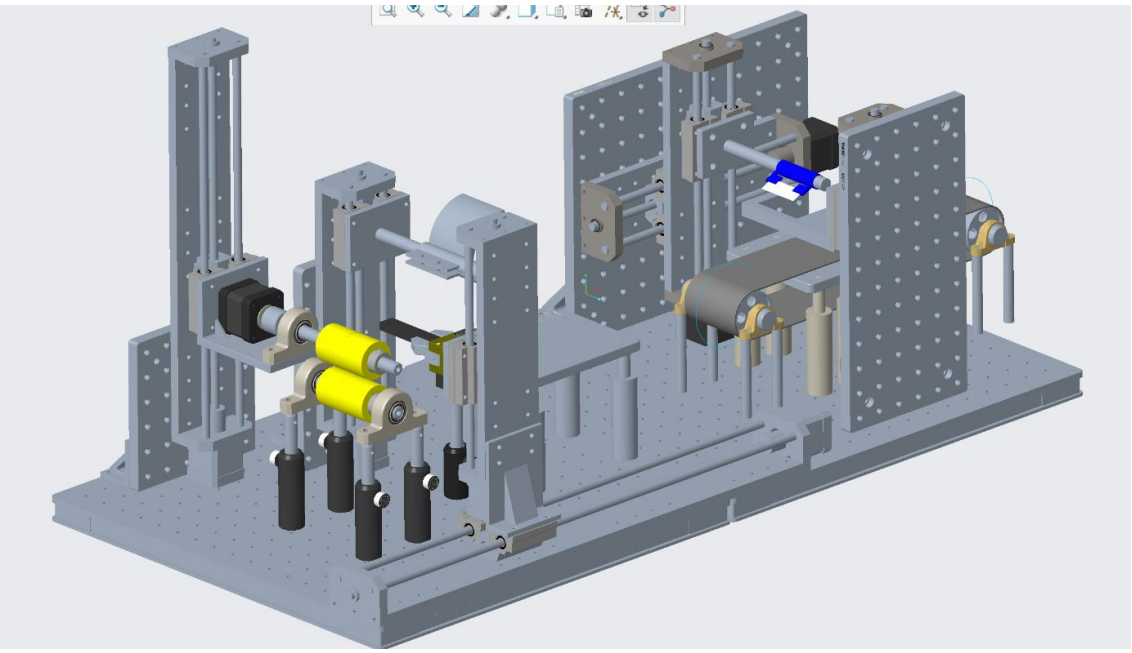

Figure 28. 3D modeling of tape-peeling and unrolling stage

2.1 Tape Peeling Stage

Tape peeling stage is designed to scrape tapes from cores. The cores from various cell supplier have different tape positions (Figure 29): some tapes are attached in the middle of cores while others are placed on the edge of cores, and variations also exists in shapes and sizes of tapes. The goal of tape peeling stage is to scrape the different tapes with various position from cores.

Figure 30 shows the 3D model of the designed tape peeling stage. The main idea of design is using the blade to peel the tape. The system includes a conveyor belt, a support plate, an upper plate and a blade. The conveyor belt transfers the cores to the peeling stage. The upper plate which has one freedom (Z direction) moves down to fix the position of cores while the support plate stands the force from the upper plate and holds cores. The blade which have two degree of freedom (Z and Y direction) first moves down and then moves forward to scrape the tapes from cores. Figure 31 shows the process of tape peeling steps.

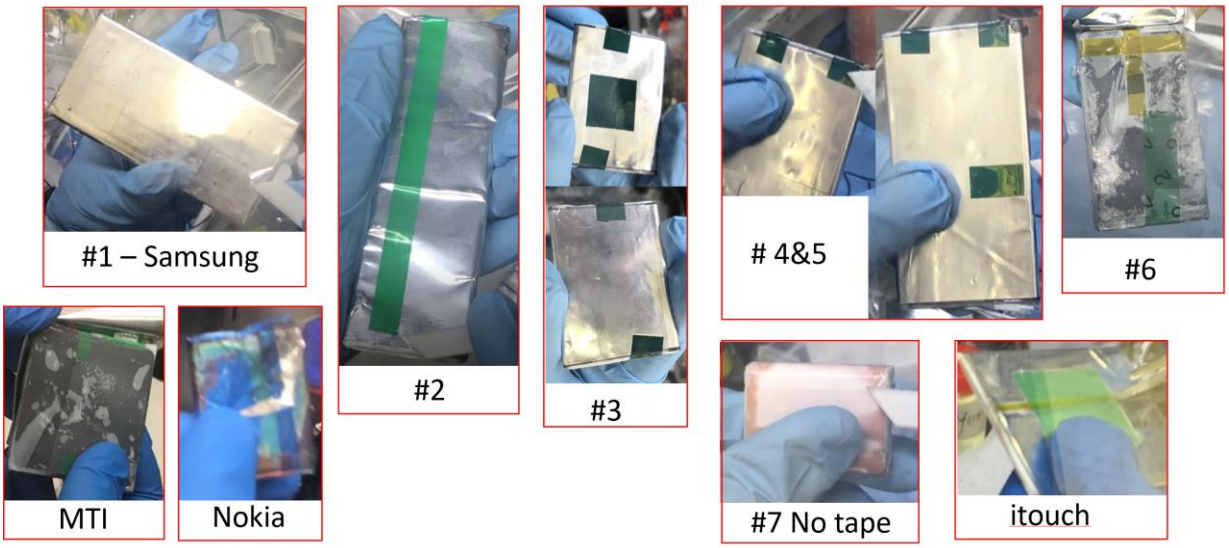

Figure 29. Tape position of different type of cores

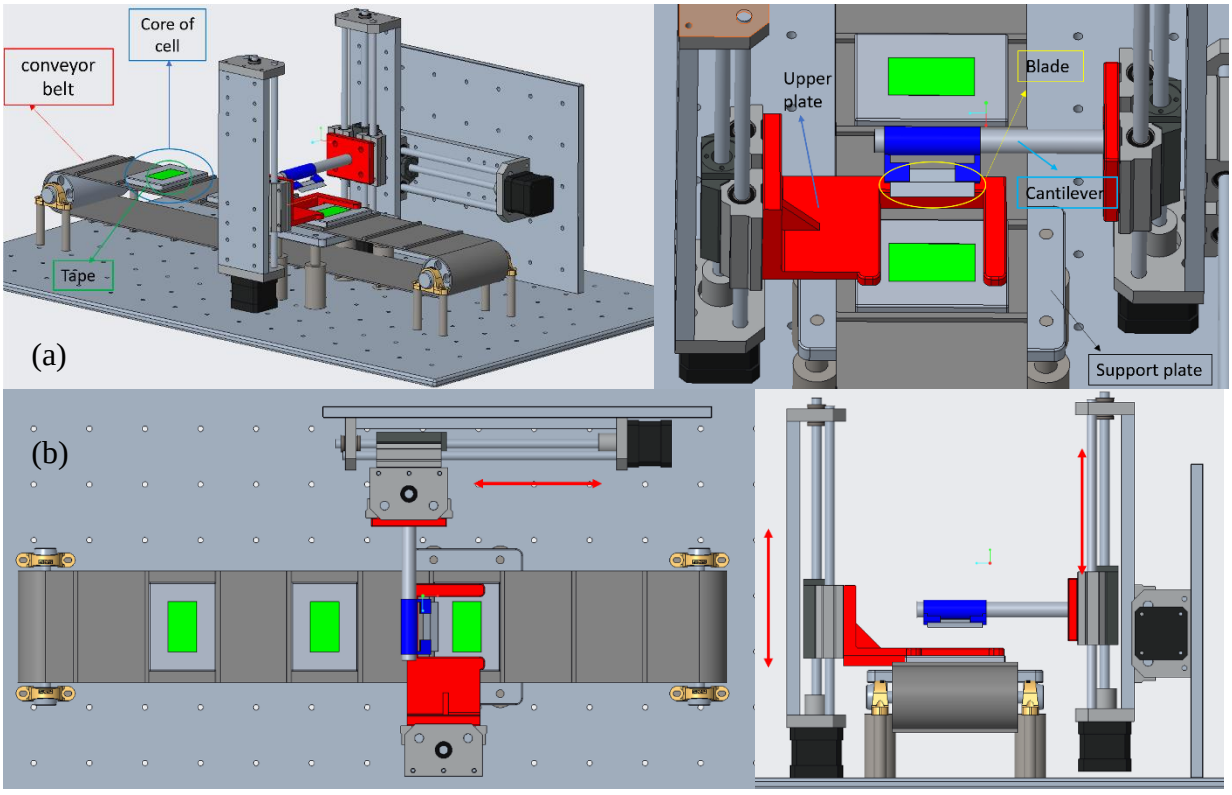

Figure 30. (a)The 3D model of the tape peeling stages and (b) The moving motion of each components

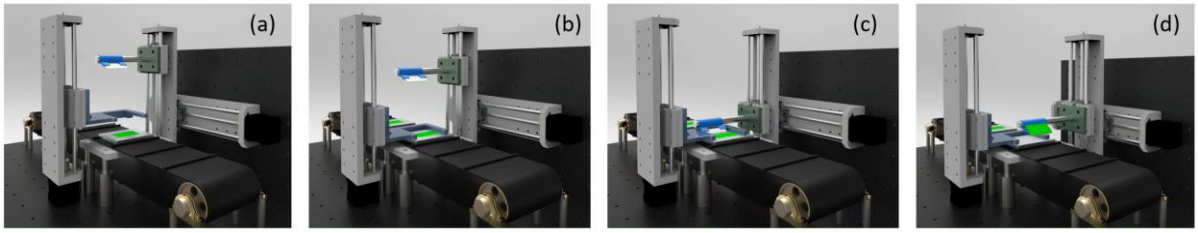

Figure 31. The mimic process of tape peeling:(a) transfers cores to the peeling stage, (b) upper plate move down to fix the position (c) the blade move down and (d) scrape the tapes from cores.

However, the system is not able to scrape the edge tape because the upper plate prevents the blade reach the edge. Figure 32 shows the real stage build with the improvement. The upper plate is deleted, and a barrier is added to fix the position of cores. A spring is also added in the system to deal with the various thickness of cores. Figure 33 shows the peeling process of the real stage.

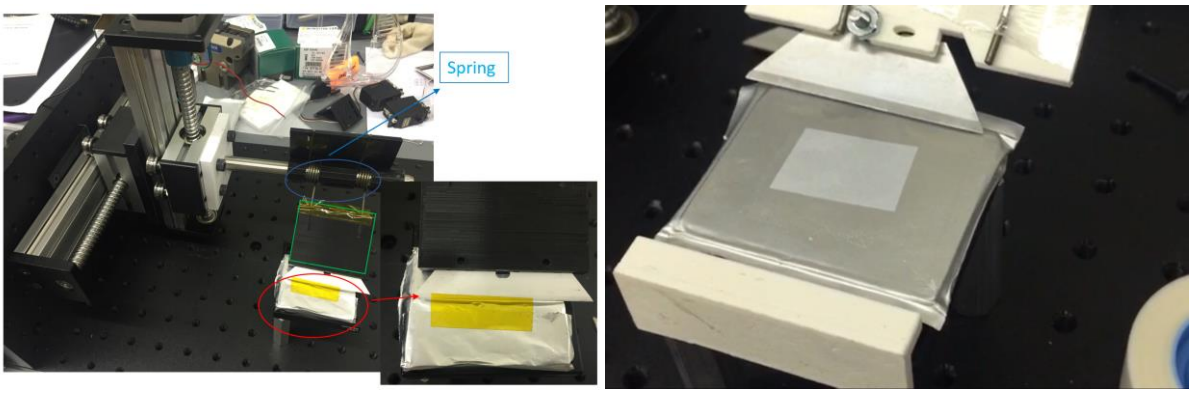

Figure 32. Real tape-peeling stage with improvement

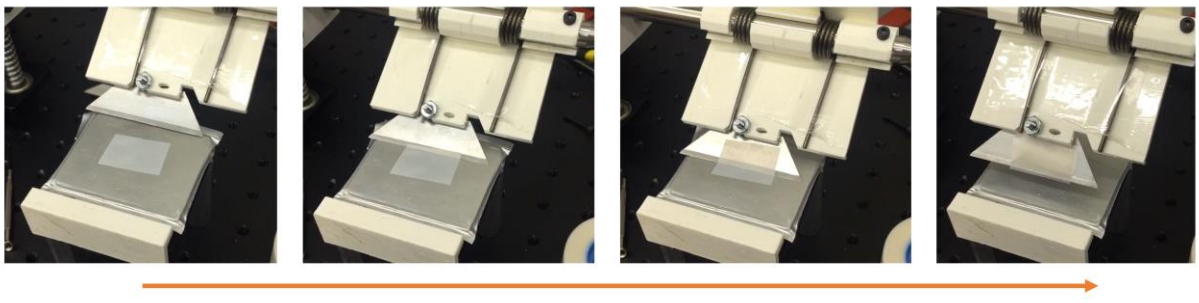

Figure 33.Real tape peeling process

2.2 Unrolling stage

The unrolling stage is designed for the prismatic winding cores. Unrolling is a key process before sorting stage of prismatic winding core. The purpose is unrolling cores to prepare for sorting process. The first idea of unrolling is using a mandrel to be inserted into centers of cores and rotating the mandrel to unrolled cores. The computer vision is used to find the center of cores. However, the layers are closed to each other which increase the difficulty in the processing. To reach high successful rate, the system needs an accurate computer vision system which can exactly find the position of center and a precise stepper motor that can accurate move the mandrel to the center of cores. Thus, the design is changed. The new idea is based on the human motion when unrolling cores.

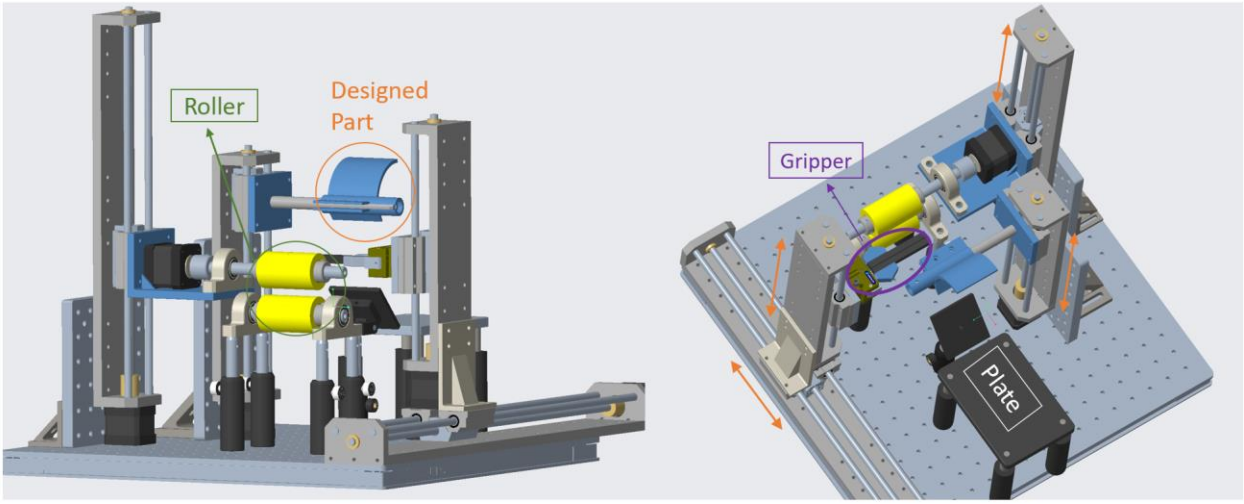

Figure 34. 3D CAD model of Unrolling System

Figure 34 demonstrates the 3D model of the unrolling stage. The stage includes a plate, a gripper, rollers and a key designed part. The griper which have two degrees (Z and Y direction) of freedom clamps cores and load cores on the stage. The designed part which has one degree of freedom (Z-direction) moves down. The upper roller which has one degree of freedom (Z-

direction) moves down and rotates to provide forward force. With the designed part, cores can rotate themselves by only forward force provided by roller. Figure 35 shows the real build stages and Figure 36 displays the real unrolling process.

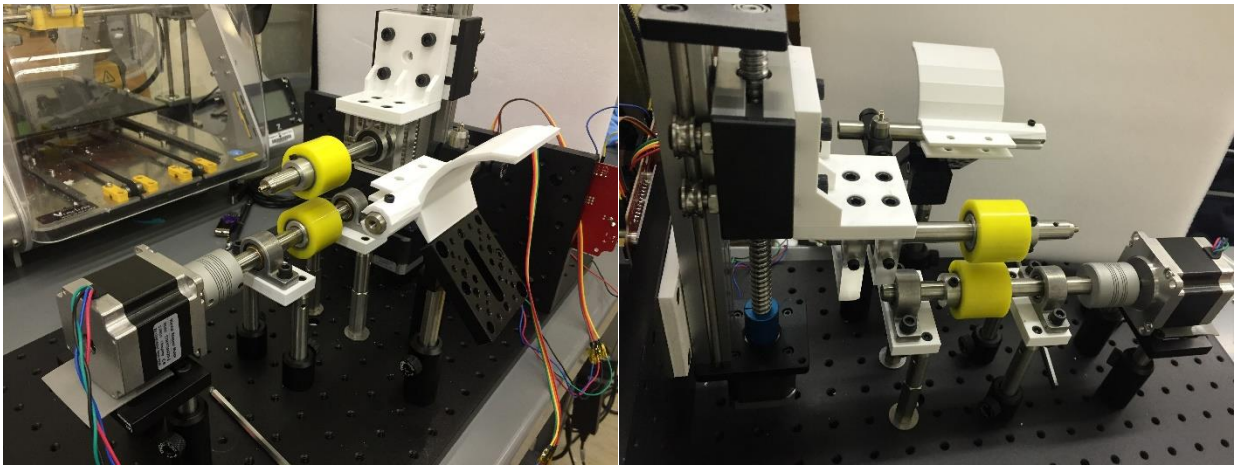

Figure 35. The real built unrolling stage

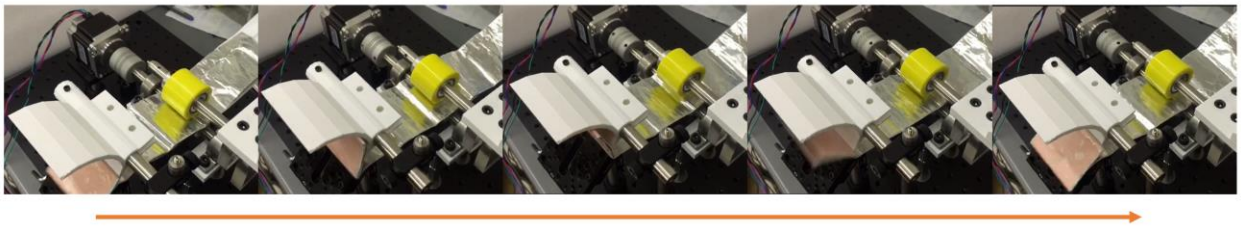

Figure 36. The real unrolling processes

Chapter 3: Recycling of cathode materials

3.1 Materials and Experiments

3.1.1 Li:Co Ratio by Inductively Coupled Plasma (ICP)

Instruments

The ratio of Li and Co in Li_xCoO_2 could be tested by Inductively Coupled Plasma. The instrument used is Inductively Coupled Plasma Atomic Emission Spectrometer (ICP-AES) provided by Soil Lab in Virginia Tech. The ICP instrument is a Spectro ARCOS SOP (Side-On [or radial view of the] Plasma interface) made by Spectro Analytical Instruments, Inc.

Sample preparation

The first step to prepare samples is dissolving the LCO into solution. The diluted 34% Hydrochloric acid (HCl), 30% Hydrogen peroxide (H_2O_2) and DI water are used to make the solution. Then 4mg powder of samples are measured and solved into acid solution. Next, the solution is put into the convection oven, and heated at 70°C for one day. After heating, the acid solution is diluted to be 0.467% acid concentration with well-string.

3.1.2 XRD and SEM

The XRD patterns of products are measured by a bench-top X-ray diffractometer (Bruker, D2 PHASER). The scanning rate is 0.06°/s and the 2θ range is from 15° to 80° (Cu Kα radiation, 40kV, 30mA, λ = 1.5418 Å). The SEM images are taken from FEI Quanta 600 FEG from Nanoscale Characterization and Fabrication Lab (NCFL). The FEI Quanta 600 FEG is an

environmental SEM that can be operated in high-vacuum and low-vacuum modes. It has a heating stage to 1000 °C and Bruker EDX with a Silicon Drifted Detector.

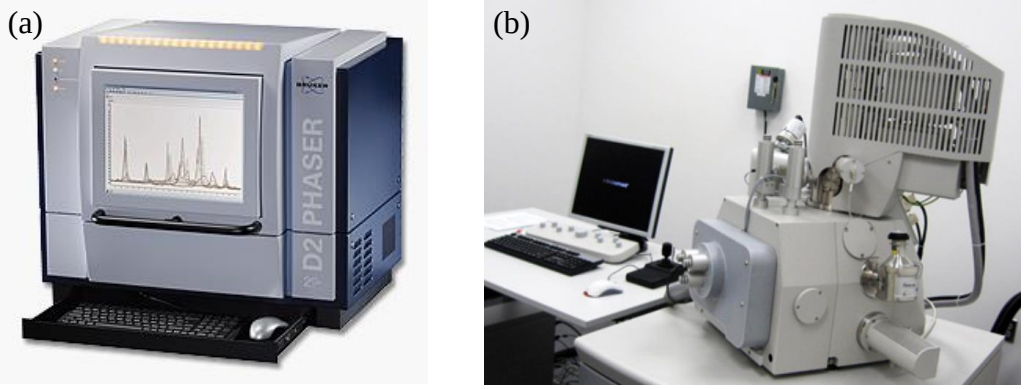

Figure 37. The image of (a) bench-top X-ray diffractometer (Bruker, D2 PHASER) and (b) SEM instrument (FEI Quanta 600 FEG)

3.1.3 EOL Materials

The EOL cathode material is retrieved from the waste batteries provided by a commercial battery collection company (Figure 38). The cathode material is identified as Li_xCoO_2 (LCO) by ICP-AES where the Li/Co ratio is around 0.92.

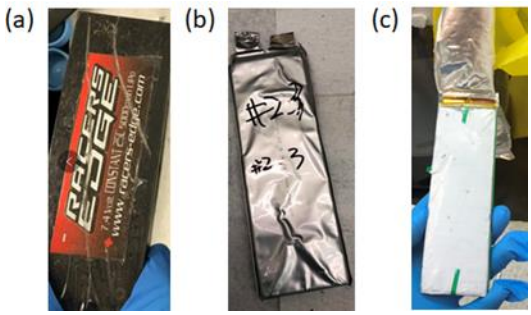

Figure 38. (a) EOL lithium-ion battery pack. (b) Individual pouch cells. (c) Cell core composed of separator, cathode material and aluminum current collector, anode material and copper current collector.

3.1.4 Sintering

Instruments

Figure 39 shows the sintering equipment: the muffle furnace (KSL-1100X, MTI corporation) and tube furnace (OTF-1200X, MTI corporation).

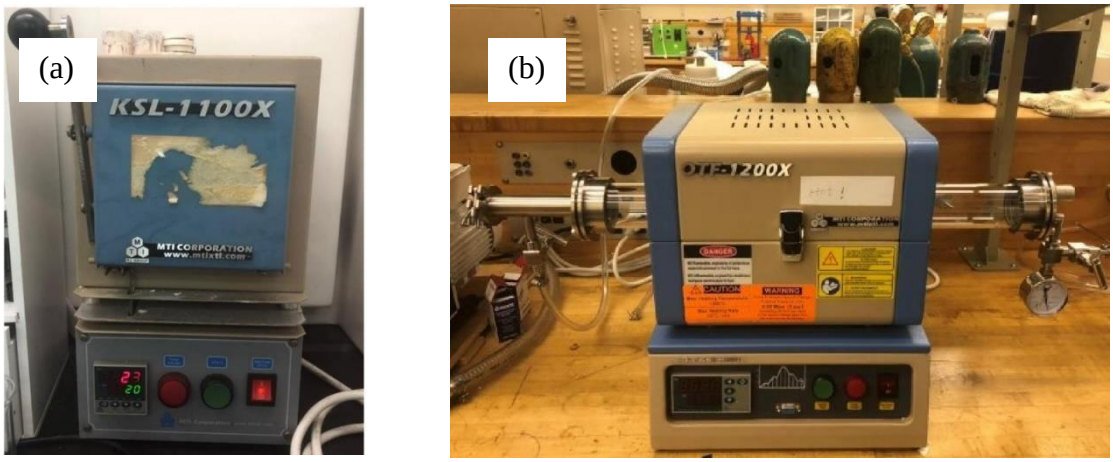

Figure 39. Instruments of sintering process: (a) Muffle furnace (b) Tube furnace

Process

EOL LCO is lithium deficient ($Li_{1-x}CoO_2$), because of lithium consuming during SEI formation and other aging mechanism. LiOH are used to add lithium and re-lithiation reaction can be represented by the following formula:

$$Li_{1-x}CoO_2 + x\ LiOH \rightarrow LiCoO_2 + x/4\ O_2 + x/2\ H_2O$$

The loss of lithium (x value) can be tested by ICP and x mole LiOH would be added to make lithium sufficient. Considering the evaporation during sintering, usually, different Li addition would be applied. For example, if the 6% of lithium is loss, we would add 4% Li, 6% Li and 8% Li (0.04, 0.06, 0.08 mole of LiOH), and sintered products are abbreviated as 4%LCO, 6%LCO, 8%LCO. Figure 40 shows the process of preparing sintering samples.

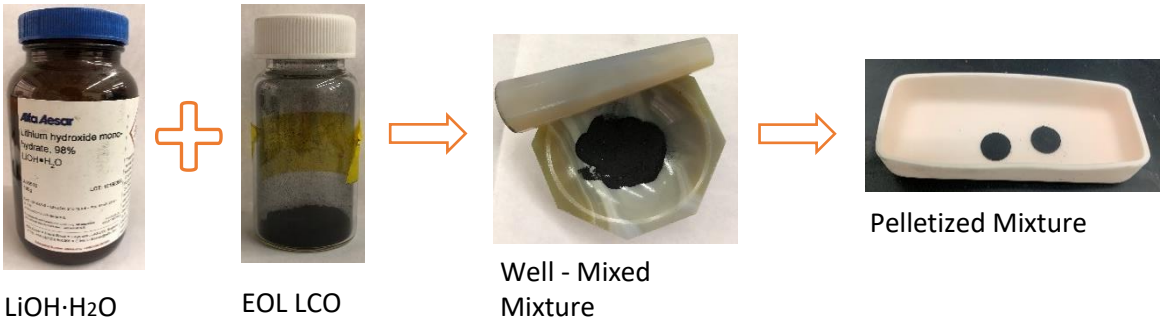

Figure 40. Process of preparing samples for sintering

To investigate the impact of the amount of lithium addition on the final recycled products, the EOL cathode material Li_xCoO_2 is first mixed with LiOH and pressed into pellets with the mole ratios of $LiOH/Li_xCoO_2$ to be 4%, 6%, 8%, 10% and 12%. To study the temperature and atmosphere effects, the pelletized mixture is sintered at different temperature (500 °C and 700 °C) and for 12 hours in both air and O_2. The O_2 which is stronger oxidant can promote the oxidization process of impurity (carbon and binder) in EOL LCO. Table 1 shows sintering conditions for each sample.

Table 1. Sintering conditions of each sample

Sample	Li addition	Temperature	Time	Atmosphere
#1	6%	700 °C	12 h	Air
#2	8%			
#3	10%			
#4	12%			
#5	4%	500 °C	12 h	Air
#6	6%			
#7	8%			
#8	4%	500 °C	12 h	O_2
#9	6%			
#10	8%			

The samples from #1 to #7 are sintered in the air by using the muffle furnace in Figure 39(a) and samples from #8 to #10 are sintered in the O_2 by using tube furnace in Figure 39(b).

3.1.5 Electrode Prepares and Coin Cell Assemble

The commercial $LiCoO_2$ used for benchmark is purchased from Sigma. Figure 41 displays the electrode preparation process. The slurry is made first by dry-mixing the weighted active materials and the weighted Timical Carbon as the conductivity in the mortar. Then well prepared 5% PVdF/NMP solution is weighted and added into mortar. The ratio of active material, carbon and PVdF is 8:1:1 in weight. Slurry need to be well mixed and should be coated on the Al foil by the blade (200μm). The Timical Carbon, the PVdF are all purchased from MTI corporation. After slurry coating on the Al foil, slurry would first be dried in the convection oven for 3 hours at 60°C, and then cut into small rounds (electrodes) with 14mm diameter. Finally, the round electrodes would be dried in the vacuum oven for 12 hours at 65°C.

Figure 41.Process of slurry and electrodes preparation

After electrodes are prepared, the next step is making coin cells. Figure 42 shows the components of a coin cell. To test the property of products, the half cells are made with Lithium chip in coin cell. The coin cell parts and electrolyte are purchase from MTI corporation: paired CR2032 button cell cases (top and bottom), made of 304 or 316 stainless steel with sealing O-ring; stainless steel wave spring (EQ-CR20WS-Spring) and spacer (15.5mm Diam x 0.5 mm-EQ-CR20-Spacer-05) for CR2032 Case; electrolyte, 1 mol/L $LiPF_6$ in EC/EMC (3:7 in volume) solution.

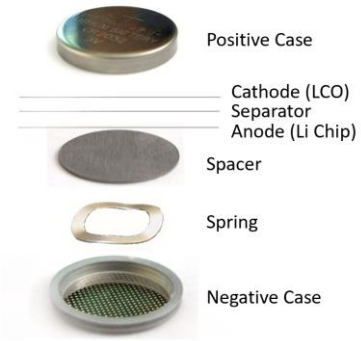

Figure 42. Components of a coin cell

3.1.6 EC Test

The assembled coin cells are tested by testers from LANHE. The test protocol is that first two cycles are tested under C/5 rate to active the cell, and then use 1C rate to run the cell until the capacity drops below 80% of original capacity. Figure 43 shows the testers from LANHE.

Figure 43. Image of testers from LANHE

3.2 Results and Analysis

3.2.1 700 °C for 12 Hours in Air

To investigate the impact of the amount of lithium addition on the final recycled products, the EOL cathode material Li_xCoO_2 is first mixed with LiOH and pressed into pellets with the mole ratios of $LiOH/Li_xCoO_2$ to be 6%, 8%, 10% and 12% (abbreviated as 6%LCO, 8%LCO, 10%LCO and 12%LCO). Then the pelletized mixture is sintered at 700 °C for 12 hours in air.

Materials characterization of EOL and recycled cathode materials

The ICP results show that the Li/Co ratios of 6%LCO, 8%LCO, 10%LCO and 12%LCO are 1.010, 1.024, 1.029 and 1.042. The Li/Co in the products after sintering increases with the increasing lithium addition. Figure 44 shows the XRD patterns of EOL cathode materials, 6%LCO, 8%LCO, 10%LCO and 12%LCO and as-purchased LCO from Sigma. The 104 peak of the EOL cathode shifts to the left compared to that of sintered LCO and Sigma LCO samples which indicates the lithium deficiency in the crystal structure of the EOL material. However, there is no obvious peak shift among sintered LCO and commercial LCO. Considering 6%LCO has the Li/Co ratio around 1, extra LiOH added to the initial 8%LCO, 10%LCO and 12%LCO before sintering may evaporate or form more stable Li_2CO_3 instead of intercalating into crystal structure.

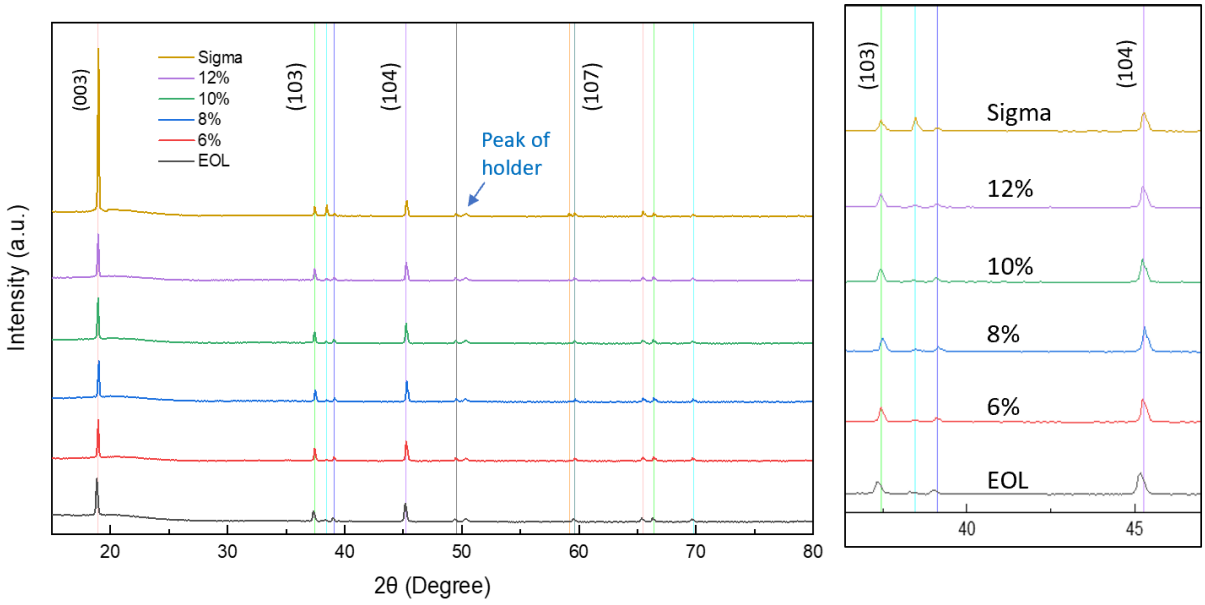

Figure 44. The XRD patterns of EOL cathode materials, sintered recycled cathode materials with 6%, 8%, 10% and 12% Li addition and as-purchased LCO from Sigma.

Figure 45 shows the morphology of the EOL LCO, 6%LCO, 8%LCO, 10%LCO and 12%LCO. The primary particle size of the EOL LCO is in the range of 0.5 – 5 µm, and the secondary particle size is around 10 µm. After sintering, there is no obvious change in particles size except that the edges of particle become sharper possibly due to the crystal growth and at high temperature and decomposition of residual binder/carbon

(a) EOL LCO

(b) 700 °C 6%LCO Air

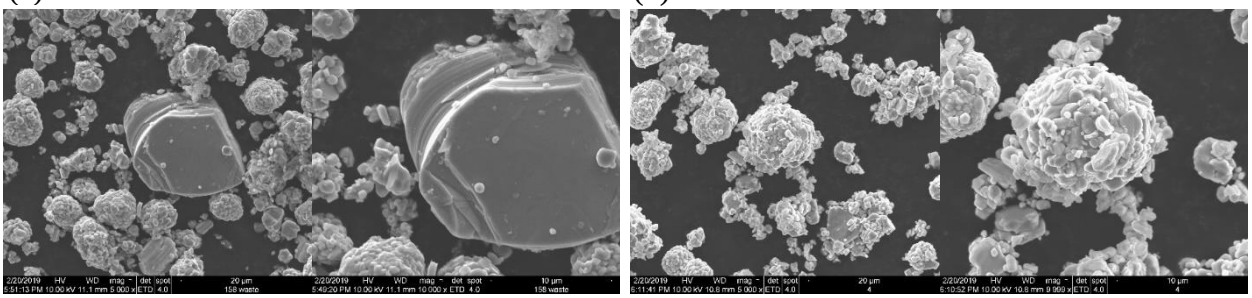

(c) 700 °C 8%LCO Air

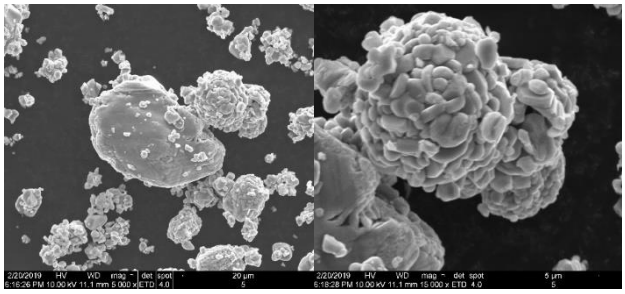

(d) 700 °C 8%LCO Air

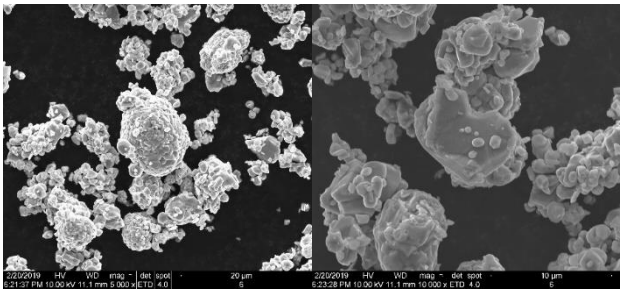

(e) 700 °C 12%LCO Air

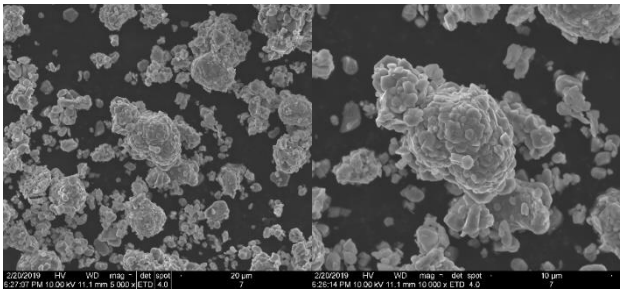

Figure 45. The SEM images of (a) EOL electrode material and sintered recycled cathode materials with (b) 6%, (c) 8%, (d) 10% and (e) 12% Li addition (700C for 12h in Air).

Electrochemical performance

Figure 46 shows that 6%LCO has higher capacity and better capacity retention than the Sigma LCO and other sintered LCO samples. The reversible capacity for the first cycle of C/5 rate of 6%LCO is around 145 mAh/g with 4.2V cutoff voltage and 183 mAh/g with 4.45V cutoff voltage. For the cells with 4.2V cutoff voltage, the capacity retention after the first 140 cycles is larger than that of Sigma LCO, although after 150 cycles, the capacity drops dramatically. For the cells with 4.45V cutoff voltage, the capacity retention is still 145 mAh/g after 140 cycles which is much better than the other tested samples. For cells with 8%LCO, 10%LCO and 12%LCO, the EC performances are similar and all of them have worse performance than 6%

LCO possibly due to the lithium excess across all of them. The data is repeatable, see more results in Appendix A.

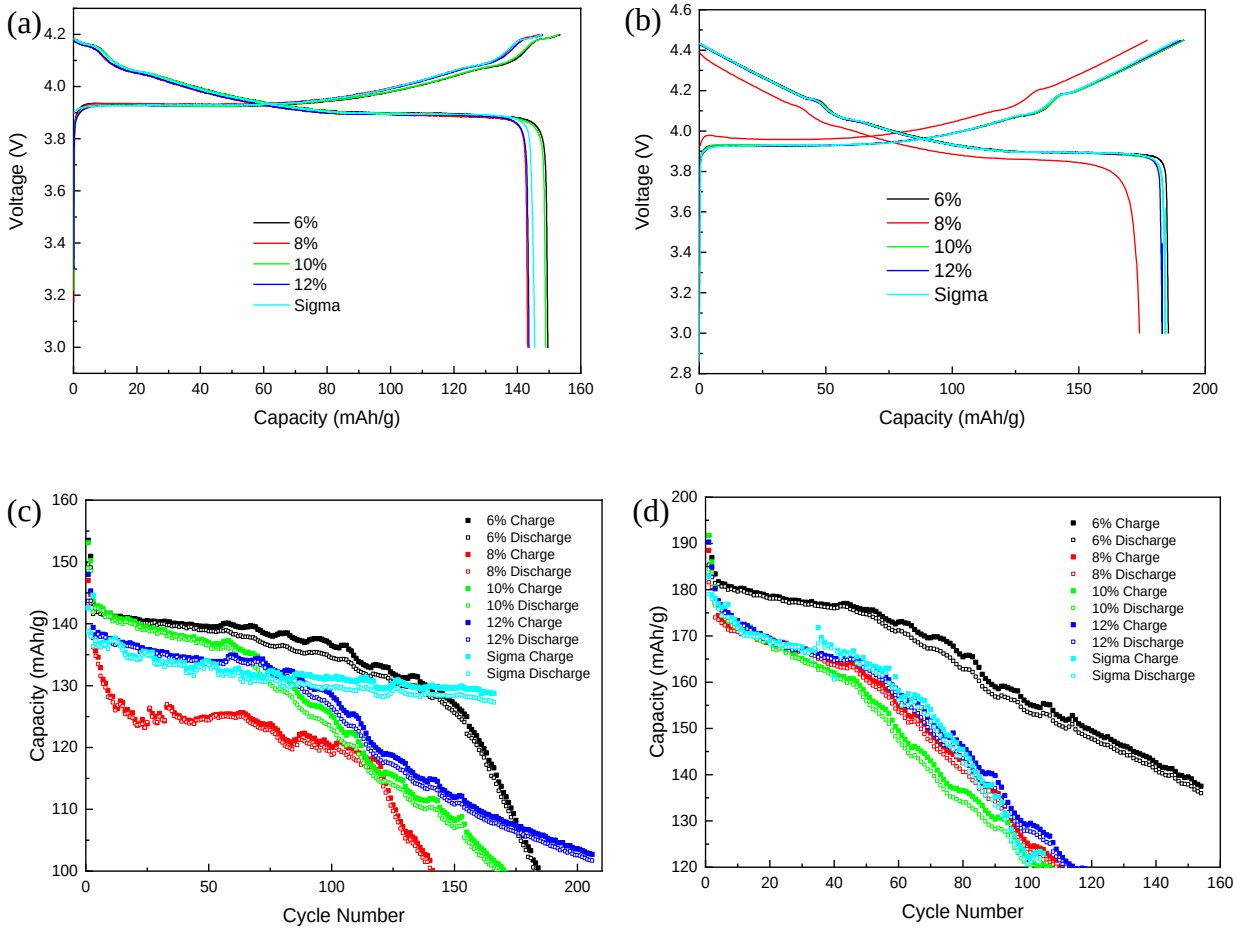

Figure 46. The charge/discharge voltage profiles of sintered recycled cathode materials with 6%, 8%, 10% and 12% Li addition and as-purchased LCO from Sigma at C/5 rate cycling between (a) 3-4.2V and (b) 3-4.45V. The cycling performance of sintered recycled cathode materials with 6%, 8%, 10% and 12% Li addition and as-purchased LCO from Sigma at C rate between (c) 3-4.2V and (d) 3-4.45V.

3.2.2 300 °C for 12 Hours in Air

To save input energy for recycling, the low-temperature sintering conditions are applied to see if the characterization and EC performance of sintered products would maintain same. 300 ℃ air sintering is applied. The EOL cathode material Li_xCoO_2 are mixed with LiOH and pressed into pellets with ratios of LiOH/ Li_xCoO_2 to be 4%, 6% and 8% and sintered in 300 ℃ for 12 hours in air.

After sintering, the white particles appeared in the sintered products, although LiOH and EOL materials are mixed well before sintering. The white particles increased when more LiOH added before sintering (Figure 47). The white particles may be the re-crystallized LiOH since the 300°C is below the melting point of LiOH, which means that the Li is not intercalate into crystal structure.

(a)  (b) 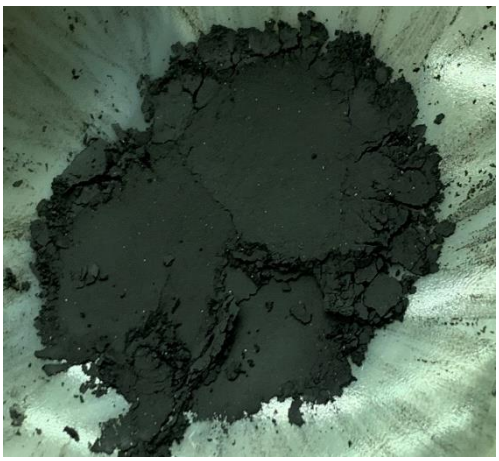

Figure 47. Products after sintering in 300°C for 12h with (a) 6% and (b) 8% Li addition

Figure 48 shows the SEM results. There is not obvious difference between the particle size, but for particle sintered at 300 ℃, the surface is not smooth. The thin and rough covers appear on the particle surface, which may be caused by un-melting LiOH. Since the products' characterizations are not good, so the EC performances are not tested for 300 ℃ sintered products.

(a)

300 °C 4%

Air

(b)

300 °C 6%

Air

(c)

300 °C 8%

Air

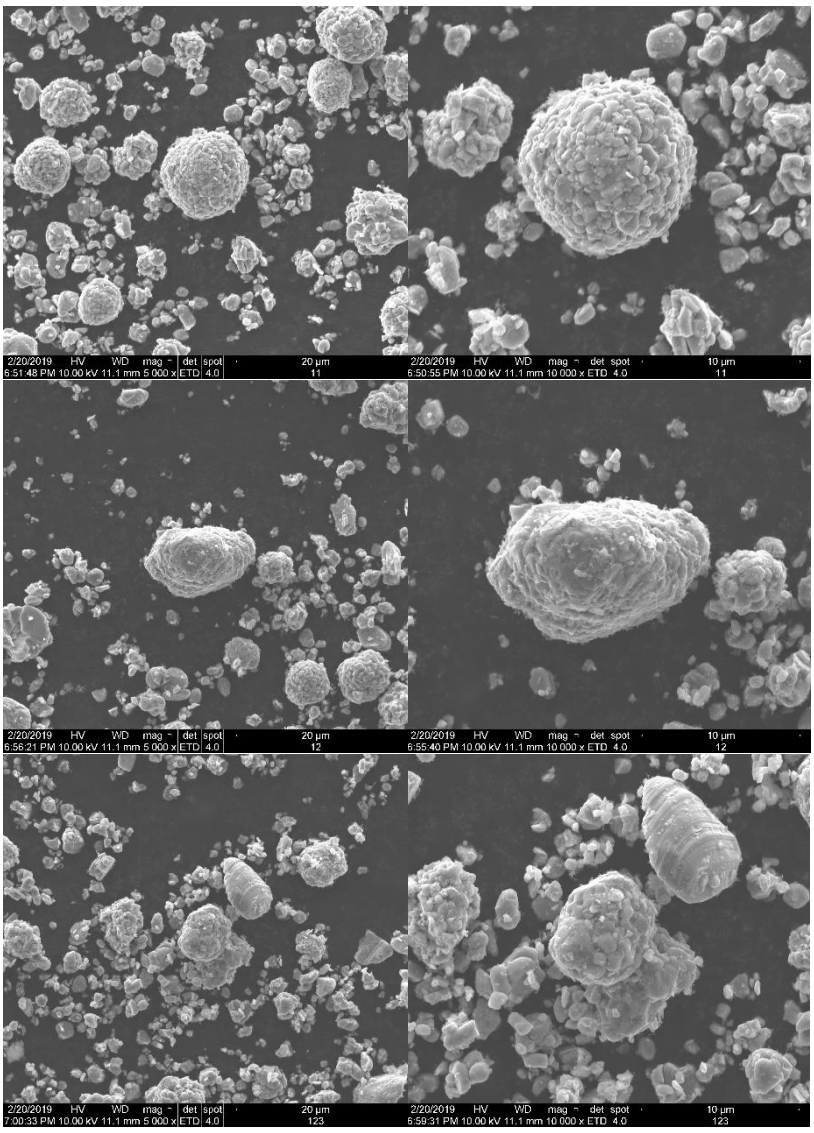

Figure 48. SEM image of 300C sintered products with (a) 4%LCO (b)6% LCO and (c) 8% LCO

3.2.3 500 °C for 12 Hours in Air

Since the results of products sintered at 300 °C are not acceptable, 500 °C air-sintering is applied to EOL LCO with same method.

Materials characterization

The ICP results show that the Li/Co ratios of 4%LCO, 6%LCO and 8%LCO are 0.981, 1.002 and 1.011. Also, the Li/Co in the products after sintering increases with the increasing lithium addition. Figure 49 shows the XRD patterns of EOL cathode materials, 4%LCO, 6%LCO, and 8%LCO and as-purchased LCO from Sigma. The results are same that the 104 peak of the EOL cathode shifts to the left compared to that of sintered LCO and Sigma LCO samples, indicating the lithium deficiency in the crystal structure of the EOL material. To compare the XRD results among different sintering temperature, Figure 50 displays the comparison XRD results for 6%LCO sintered in 500 °C and 700 °C in air. There is no obvious peak shift among 6%LCO with different temperature, same for 8%LCO.

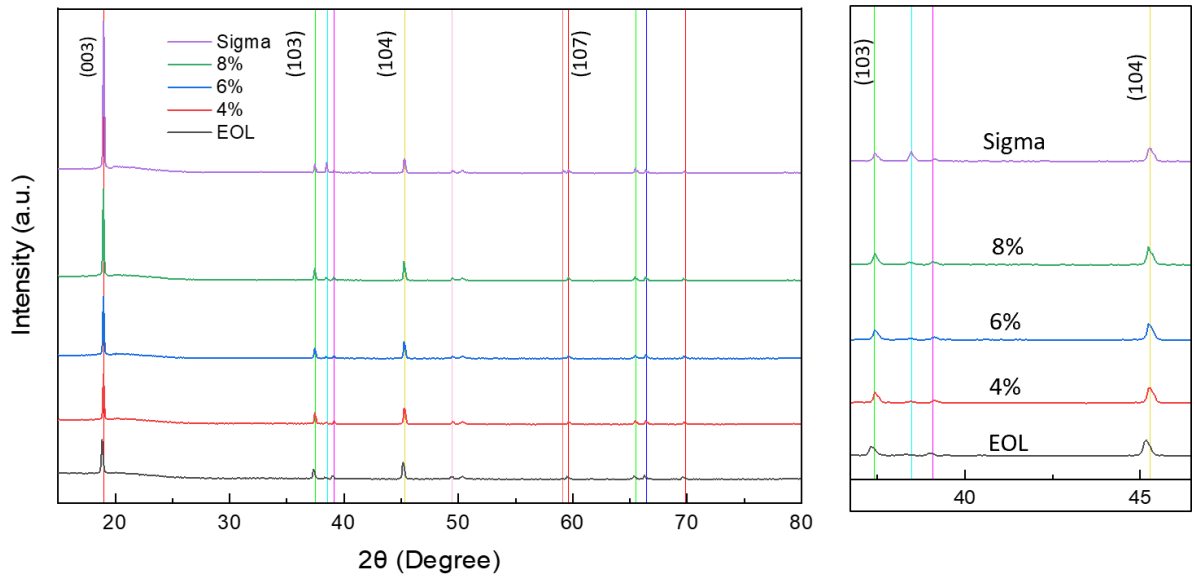

Figure 49. The XRD patterns of EOL cathode materials, sintered recycled cathode materials with 4%, 6% and 8% Li addition and as-purchased LCO from Sigma.

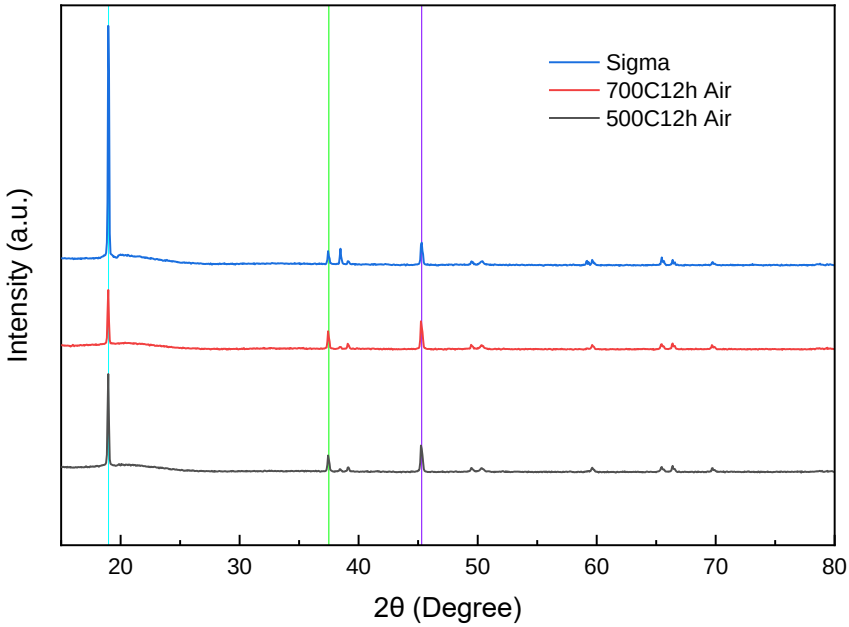

Figure 50.The XRD patterns of EOL cathode materials, 700 ℃ and 500 ℃ sintered recycled cathode materials with 6% Li addition and as-purchased LCO from Sigma.

Figure 51 shows the morphology of the EOL LCO, 4%LCO, 6%LCO and 8%LCO. After sintering at 500 ℃ for 12h in air, there is no obvious difference in particles size compare to the products sintered in 700℃ (Figure 51), and all the surfaces are smooth.

(a)

500 °C 4%

Air

(b)

500 °C 6%

Air

(c)

500 °C 8%

Air

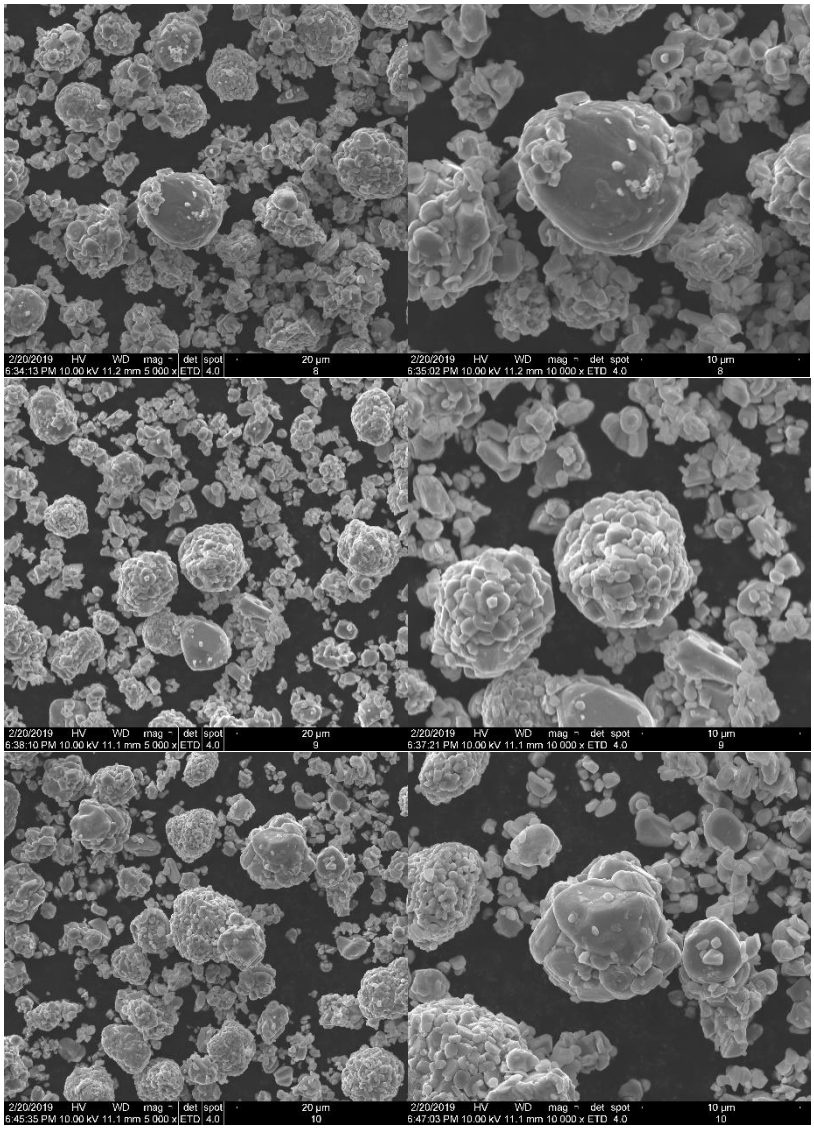

Figure 51.SEM image of 500C sintered products with (a) 4%LCO (b)6% LCO and (c) 8% LCO

Electrochemical performance

For EC performance of material sintered at 500°C, it's hard to get conclusion about which lithium addition is better (Figure 52). Although the average capacity is lower than material sintered at 700°C, most of materials have better cycling performance than Sigma LCO. The capacity of first cycle of C/5 rate increases with increasing lithium addition for both 4.2V and

4.45V cutoff voltage. The reversible capacity for the first cycle of C/5 rate of 6%LCO is around 140 mAh/g with 4.2V cutoff voltage and 180 mAh/g with 4.45V cutoff voltage.

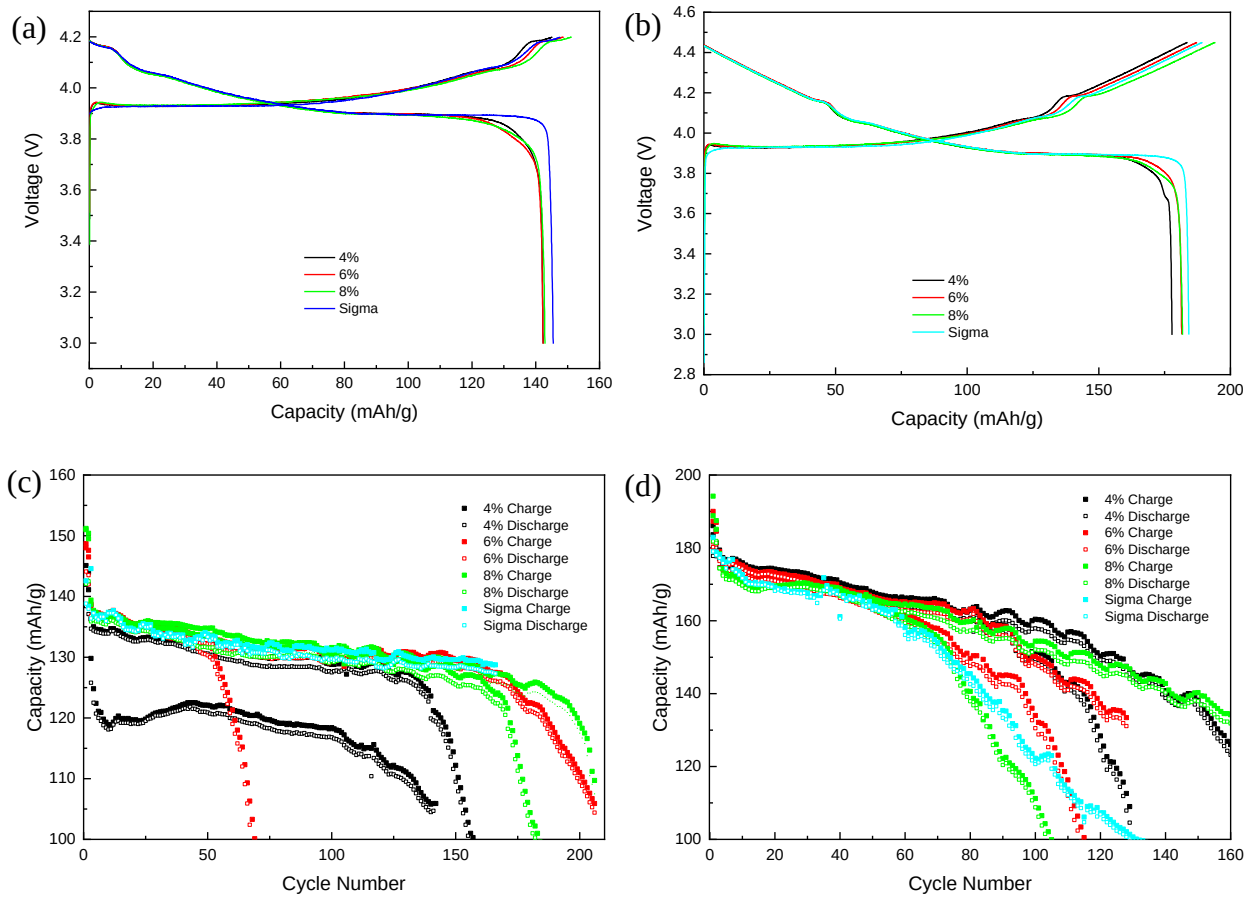

Figure 52. The charge/discharge voltage profiles of sintered recycled cathode materials with 4%, 6% and 8% Li addition and as-purchased LCO from Sigma at C/5 rate cycling between (a) 3-4.2V and (b) 3-4.45V. The cycling performance of sintered recycled cathode materials with 4%, 6% and 8% Li addition and as-purchased LCO from Sigma at C rate between (c) 3-4.2V and (d) 3-4.45V.

3.2.4 500 °C for 12 Hours in O_2

Because the products sintered at 500 °C in air don't have results as good as 700 °C in air, another group of experiments is added to investigate the impact of the sintering atmosphere to final recycled products. Same method to make pellets with mole ratios of $LiOH/Li_xCoO_2$ to be 4%,

6% and 8%, but sintered at 500 °C for 12 hours in the pure O_2 by using tube furnace show in Figure 24(b).

Materials characterization

The ICP results show that the Li/Co ratios of 4%LCO, 6%LCO and 8%LCO are 0.976, 1.003 and 1.016. Also, the Li/Co in the products after sintering increases with the increasing lithium addition. Figure 53 shows the XRD patterns of EOL cathode materials, 4%LCO, 6%LCO, and 8%LCO sintered at 500 °C in O_2 and as-purchased LCO from Sigma. The results are also same that the 104 peak of the sintered LCO shifts to the right compared to that of EOL LCO, indicating lithium intercalate into the crystal structure of the EOL material.

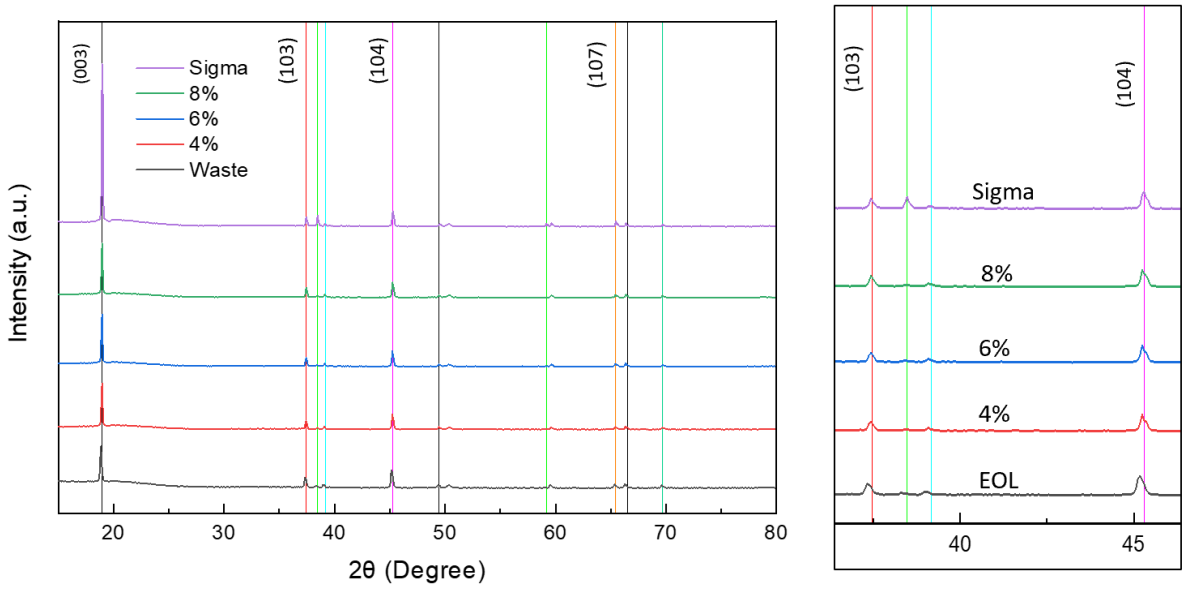

Figure 53. The XRD patterns of EOL cathode materials, sintered recycled cathode materials with 4%, 6% and 8% Li addition and as-purchased LCO from Sigma.

Figure 54 shows the SEM image of products sintered at 500 °C in O_2. There is no obvious change of particle size and the surfaces are also smooth.

(a)

500 °C 4%

O2

(b)

500 °C 6%

O2

(c)

500 °C 8%

O2

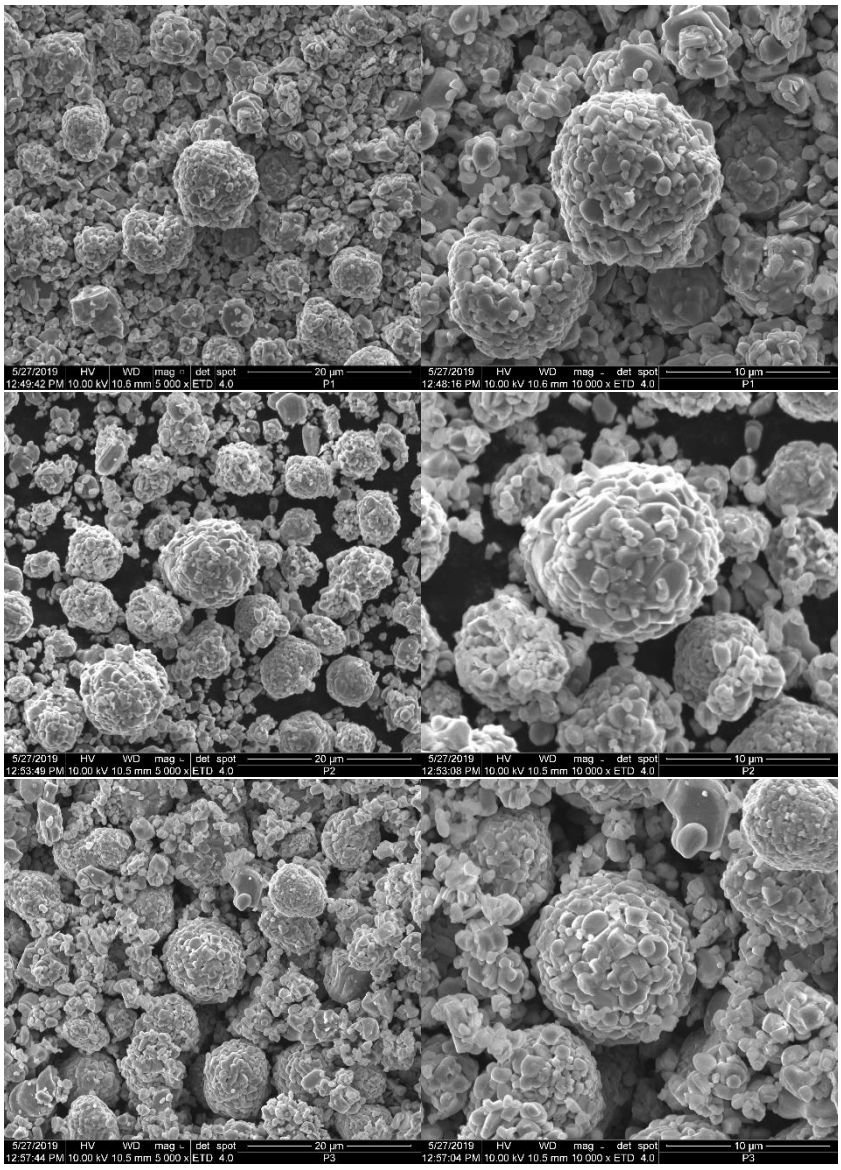

Figure 54. SEM image of 500°C O_2 sintered products with (a) 4%LCO (b)6% LCO and (c) 8% LCO

Electrochemical performance

Figure 55 displays the cycling performance of materials sintered at 500 °C in O_2. With the increasing Li addition, the first cycle (C/5) capacity increase, but cycling performance become worse. The overall capacity is a little bit lower compare to Sigma LCO with 4.2V cutoff voltage.

However, for the 4.45V cutoff voltage, although capacity of sintered materials are lower compare to capacity of sigma LCO , but sintered materials have better cycling performance.

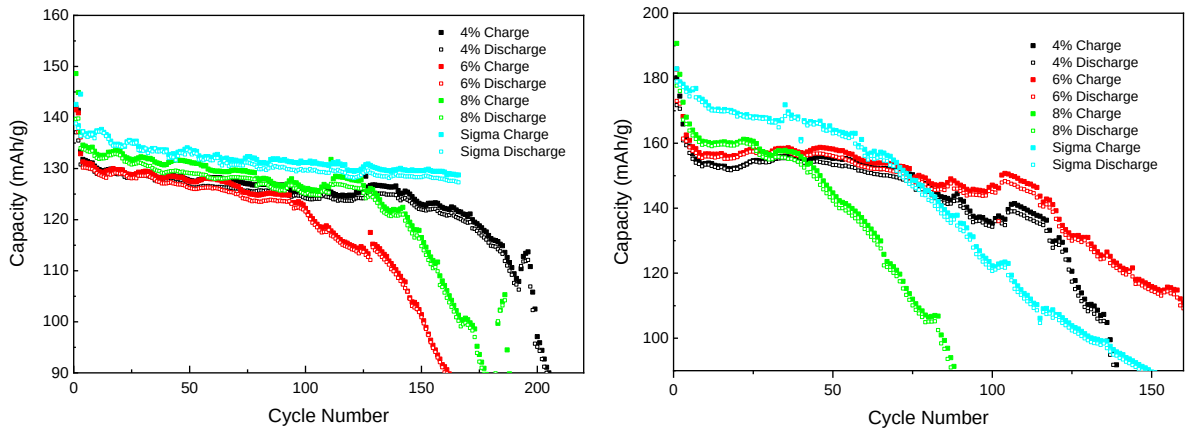

Figure 55.The cycling performance of sintered recycled cathode materials with 4%, 6% and 8% Li addition and as-purchased LCO from Sigma at C rate between (c) 3-4.2V and (d) 3-4.45V.

3.2.5 Comparison Among Different Sintering Condition

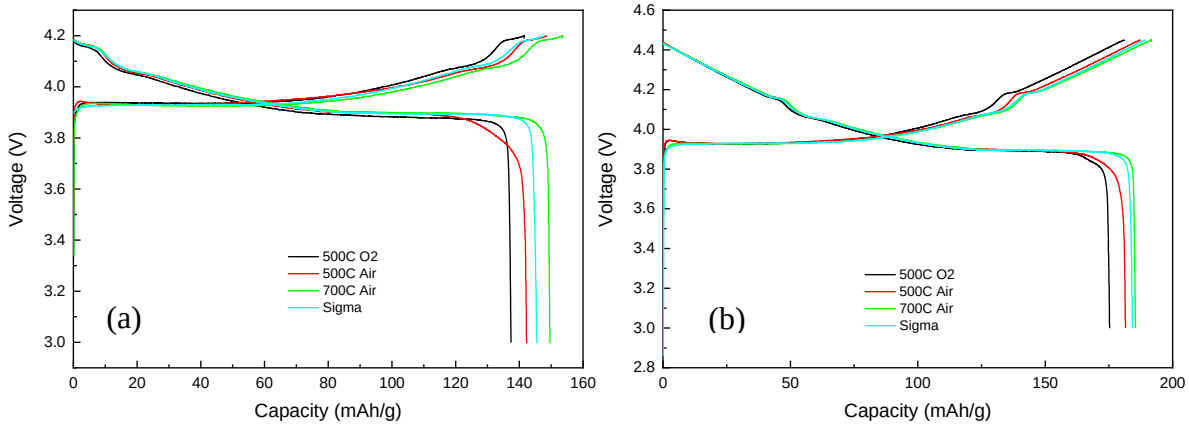

Figure 56. The first cycle (C/5 rate) charging/discharging profile of sintered materials with 6% lithium addition under (a) 3-4.2V cutoff voltage and (b) 3-4.45V cutoff voltage

Figure 56 displays the charging and discharging profile of first cycle (C/5 rate) of sintering material with 6% lithium addition. For both 4.2 and 4.45 cutoff voltage, from temperature aspect, compare 700 °C and 500 °C air sintered materials, 500 °C sintered product has lower capacity;

from atmosphere aspect, compare 500 °C air and O_2 sintered products, O_2 sintered products has lower capacity; compare with Sigma LCO, 700 °C air sintered products have higher capacity than that of sigma LCO while 500 °C air and O_2 sintered products have lower capacity than that of sigma LCO.

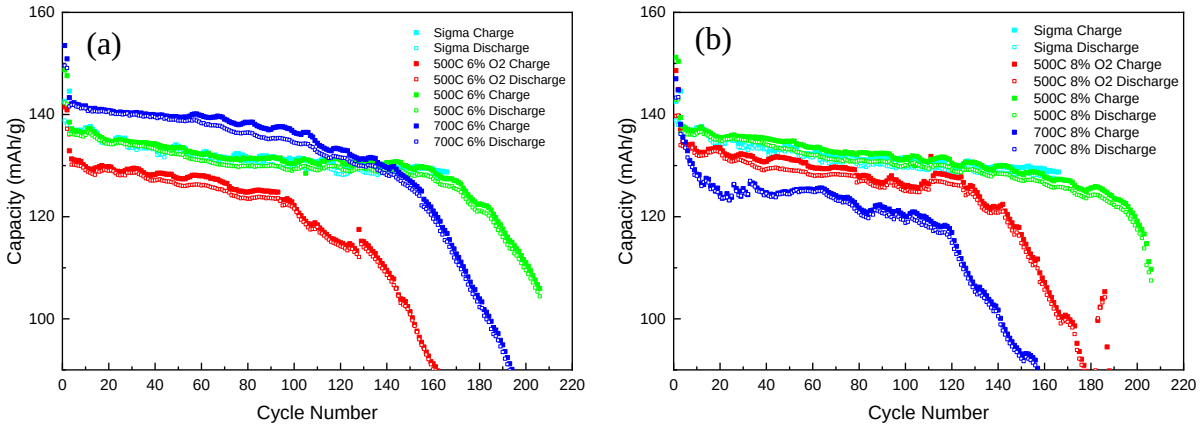

Figure 57. The cycling performance of sintered recycled cathode materials in different temperature and atmosphere with (a) 6% Li addition (b) 8% Li addition and with the 4.2V cutoff voltage

Figure 57 and Figure 58 shows the cycling performance of products with different sintering conditions. Figure 57 compares the products sintered with 6% and 8% Li addition and with 4.2V cutoff voltage. In Figure 57(a), the results show that with 6% Li addition, the higher sintering temperature applied to products, the higher capacity products have, however, products sintered at 500 °C in air have better cycling performance compare to products sintered at 700 °C in air have. Figure 57(b) displays that with 8% Li addition, the 500 °C has higher capacity and better cycling performance, the possible reason is that base on the ICP results, the 8% LCO sintered at 700 °C in air is 1.024 and for 500 °C in air is 1.011; maybe the extra Li in the structure cause the worse capacity retention. Also, being sintered in O_2 doesn't improve the performance with the cutoff voltage of 4.2V.

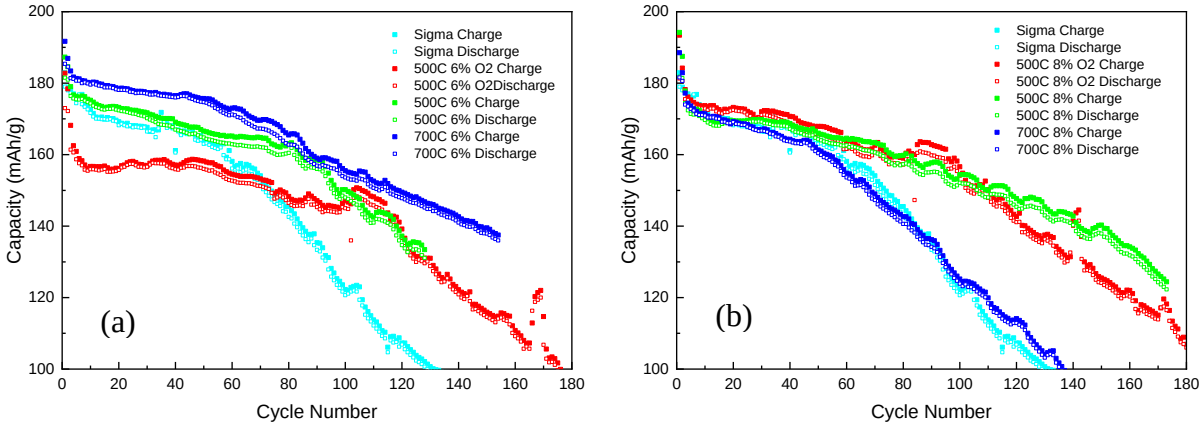

Figure 58. The cycling performance of sintered recycled cathode materials in different temperature and atmosphere with (a) 6% Li addition (b) 8% Li addition and with the 4.45V cutoff voltage

Figure 58 compare the products sintered with 6% and 8% Li addition and with 4.45V cutoff voltage. In Figure 58(a), the results show that with 6% Li addition the higher temperature, the higher capacity and better cycling performance. Figure 58(b) displays that with 8% Li addition, the 500 °C has higher capacity and better cycling performance. The reason is same that the extra Li in the structure may cause the worse capacity retention. Also, being sintered in O_2 doesn't improve the performance with the 4.45V cutoff voltage. However, comparing to the Sigma LCO, the sintered products have better capacity and cycling performance.

The results show that being sintered in O_2 doesn't improve the EC performance for both 4.2V and 4.45V cutoff voltage. The O_2 may not be helpful in the small-scale sintering. However, for large-scale sintering, if EOL LCO is pressed into large pellets, the inside impurity (like carbon and binder) can't be oxidized well in air, and O_2 which is a stronger oxidant may help oxidizing process of the impurity.

Chapter 4: Conclusion and Future Work

4.1 Conclusion

The design of using the blade to scrape the tape is feasible for tape peeling stage and the method to unrolling the prismatic winding core is achievable for unrolling stage. Different sintering conditions result in different characterizations and EC performances. For different Li additions, if the Li is excessive, the products' first cycles (C/5 rate) have higher capacity but products have worse cycling performance. For different temperature, the higher temperature (700 °C) leads to higher average capacity compare to lower temperature (500 °) if Li is not excessive, but 500 °C air sintered products have better cycling performance compare to that of 700 °C air sintered products. Sintering atmosphere has little influence on small- scale sintering. Compare to the sigma LCO, all directly recycled cathode materials have better cycling performance when cycling with 4.45V cutoff voltage. However, only 6%LCO with 700 °C air sintered products have much higher capacity when cycling with 4.2V cutoff voltage.

4.2 Future Work

In the future, more modulus should be designed for different types of core. Another group of sintering, 700°C O2 - sintering, will be applied to study how atmosphere impact on high temperature sintering. Before sintering, we can first bake the EOL LCO in the oven to burn the impurity (carbon, binder) which can help to get more accurate Li addition.

Reference

1. World Electric Vehicle Production and Lithium Demand For Electric Vehicle Batteries - 2008 through 2020 - Source Roskil. Available at: http://tommytoy.typepad.com/.a/6a0133f3a4072c970b01538f9eaae4970b-popup. (Accessed: 7th May 2018)
2. Limited, A. Stock Photo - Battery. Environmental pollution. *Alamy* Available at: https://www.alamy.com/stock-photo-battery-environmental-pollution-115408736.html. (Accessed: 7th May 2018)
3. Lv, W. *et al.* A Critical Review and Analysis on the Recycling of Spent Lithium-Ion Batteries. *ACS Sustainable Chem. Eng.* **6**, 1504–1521 (2018).
4. Reddy, T. B. *Linden's handbook of batteries*. (McGraw-Hill, 2011).
5. Zhang, Z. (John) & Ramadass, P. Lithium-Ion Batterylithium-ion batterySystems and Technologylithium-ion batterytechnology. in *Encyclopedia of Sustainability Science and Technology* (ed. Meyers, R. A.) 6122–6149 (Springer New York, 2012). doi:10.1007/978-1-4419-0851-3_663
6. Prof.Dr.-Ing Jurgen Fleischer, Prof. Dr-Ing.G. Lanza, Prof. Dr.-Ing. habil.V. Schulze. Challenges of high Quality and high-Performance Cell Stacking. wbk Institute of Production Science
7. How Thin Film Batteries Work. *AZoM.com* (2018). Available at: https://www.azom.com/article.aspx?ArticleID=15815. (Accessed: 8th May 2019)
8. Julien, C. M., Mauger, A., Zaghib, K. & Groult, H. Comparative Issues of Cathode Materials for Li-Ion Batteries. *Inorganics* **2**, 132–154 (2014).
9. Mizushima, K., Jones, P. C., Wiseman, P. J. & Goodenough, J. B. LixCoO2 (0<x<-1): A new cathode material for batteries of high energy density. *Materials Research Bulletin* **15**, 783–789 (1980).
10. Whittingham, M. S. Lithium Batteries and Cathode Materials. *Chemical Reviews* **104**, 4271–4302 (2004).
11. Zettsu, N. *et al.* Flux growth of hexagonal cylindrical $LiCoO_2$ crystals surrounded by Li-ion conducting preferential facets and their electrochemical properties studied by single-particle measurements. *Journal of Materials Chemistry A* **3**, 17016–17021 (2015).
12. Reimers, J. N. & Dahn, J. R. Electrochemical and in situ X-ray diffraction studies of lithium intercalation in Li x CoO2. *Journal of The Electrochemical Society* **139**, 2091–2097 (1992).
13. Julien, C. M., Mauger, A., Zaghib, K. & Groult, H. Comparative Issues of Cathode Materials for Li-Ion Batteries. *Inorganics* **2**, 132–154 (2014).

14. Huggins, R. A. *Advanced batteries: materials science aspects*. (Springer, 2009).

15. Vetter, J. *et al.* Ageing mechanisms in lithium-ion batteries. *Journal of Power Sources* **147**, 269–281 (2005).

16. Imhof, R. & Novák, P. In Situ Investigation of the Electrochemical Reduction of Carbonate Electrolyte Solutions at Graphite Electrodes. *J. Electrochem. Soc.* **145**, 1081–1087 (1998).

17. Wang, H., Vest, M. & Friedrich, B. Hydrometallurgical processing of Li-Ion battery scrap from electric vehicles. 16 (2011).

18. Hailey, P. & Kepler, K. Direct Recycling Technology for Plug-In Electric Vehicle Lithium-ion Battery Packs. 30 (2015).

19. Zhang, Z. *et al.* Renovation of LiCoO2 crystal structure from spent lithium ion batteries by ultrasonic hydrothermal reaction. *Res Chem Intermed* **41**, 3367–3373 (2015).

Appendix A

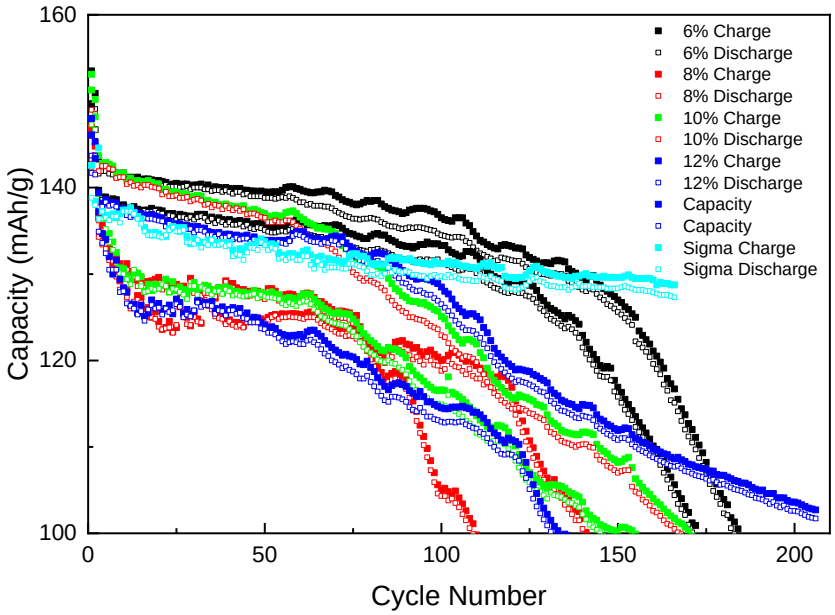

A. 1 Cycling performance of 700C12h sintered material with 4.2V cutoff voltage

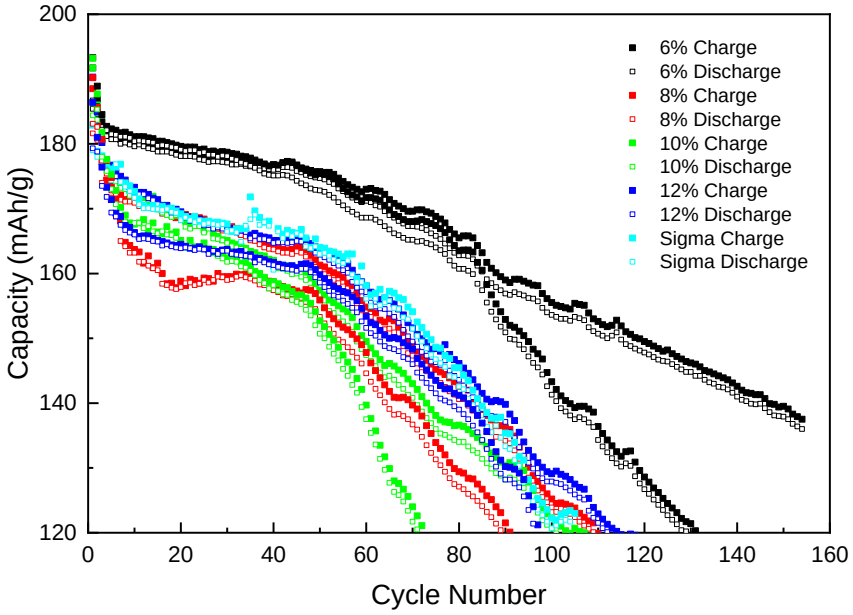

A. 2 Cycling performance of 700C12h sintered material with 4.45V cutoff voltage

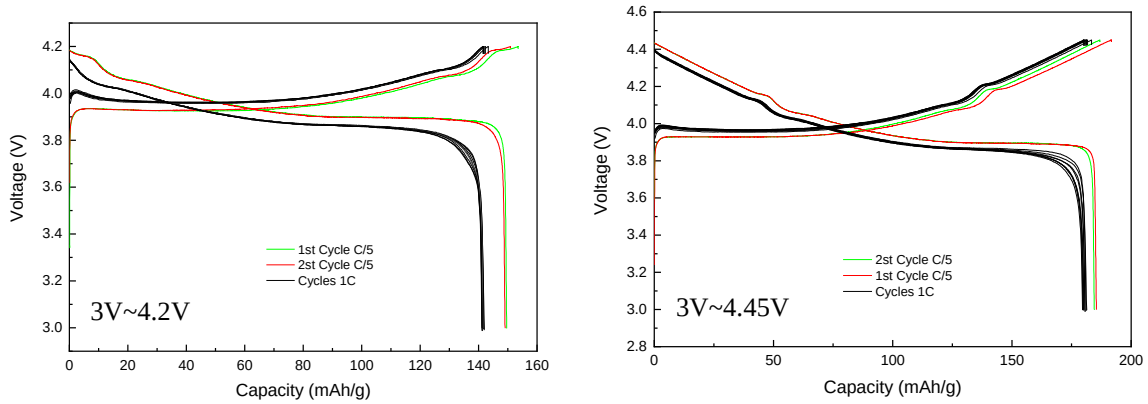

A. 3 Charging/discharging profile for 700C12h 6% Li (first 10 cycles)

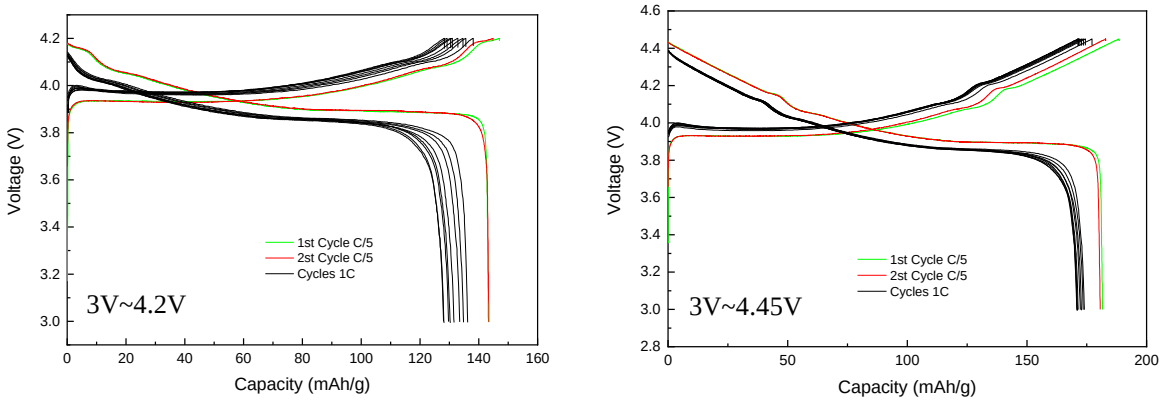

A. 4 Charging/discharging profile for 700C12h 8% Li (first 10 cycles)

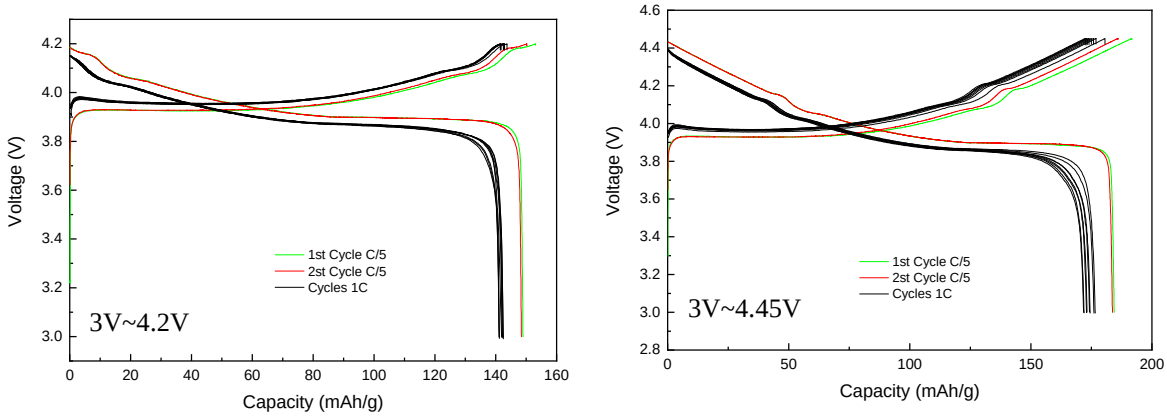

A. 5 Charging/discharging profile for 700C12h 10% Li (first 10 cycles))

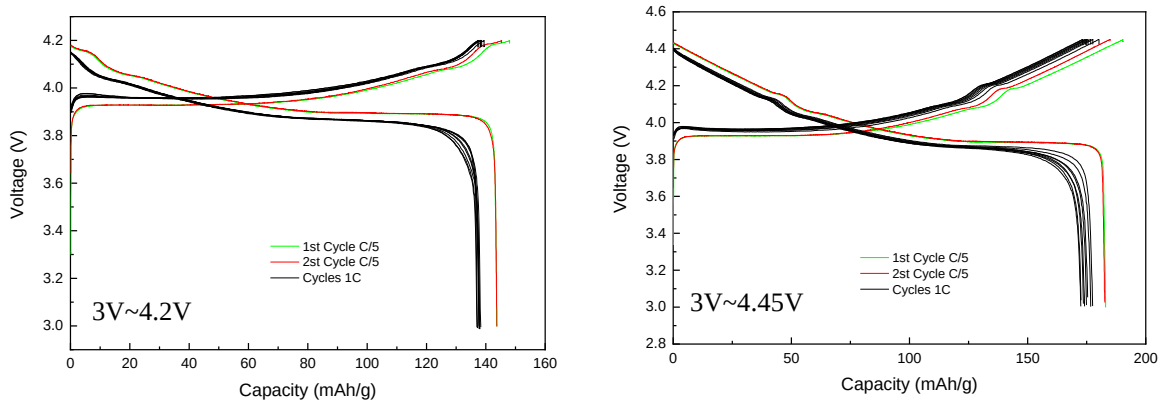

A. 6 Charging/discharging profile for 700C12h 12% Li (first 10 cycles)

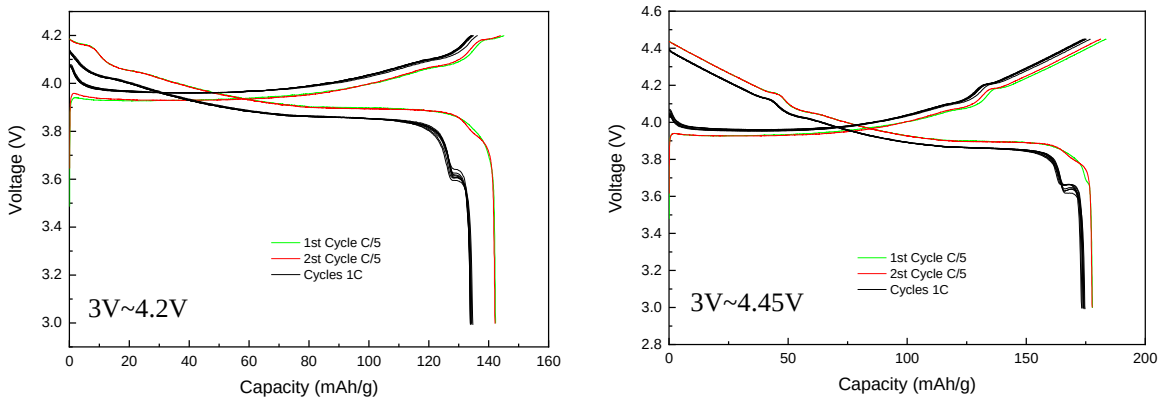

A. 7 Charging/discharging profile for 500C12h 4% Li (first 10 cycles)

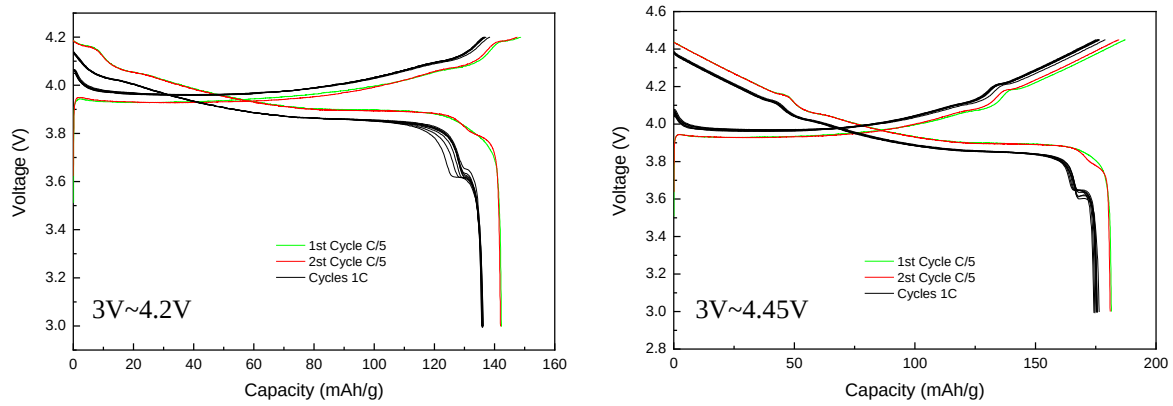

A. 8 Charging/discharging profile for 500C12h 6% Li (first 10 cycles)

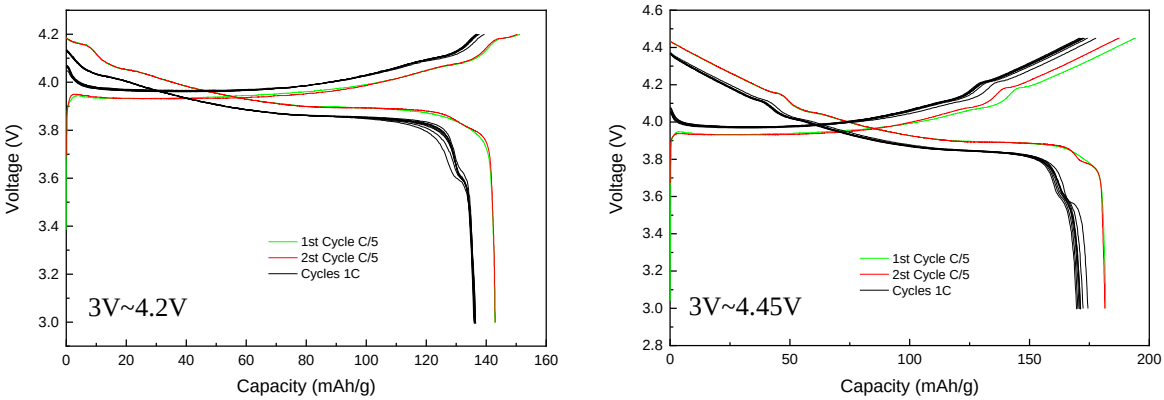

A. 9 Charging/discharging profile for 500C12h 8% Li (first 10 cycles)